ADVANCING EARTH AND SPACE SCIENCES

JGR Solid Earth

RESEARCH ARTICLE
10.1029/2024JB031017

Magnetic and Paleomagnetic Characterization of the Ivrea-Verbano Lower Crust Body (NW Italy): Assessing the Magnetization of Variscan-Age Lower Crust

Gaia Siravo[1], Fabio Speranza[1], Liliana Minelli[1], Michele Zucali[2], Eugenio Fazio[3], Chiara Caricchi[1], and Lilla Spagnuolo[1]

[1]Istituto Nazionale di Geofisica e Vulcanologia, Roma, Italy, [2]Dipartimento di Scienze Della Terra "A. Desio"—Università Degli Studi di, Milano, Italy, [3]Dipartimento di Scienze Biologiche Geologiche e Ambientali—Università Degli Studi di, Catania, Italy

Key Points:

- Magnetic, paleomagnetic and petrographic characterization of metamorphic, intrusive and ultramafic rocks from Variscan Ivrea-Verbano body
- Amphibolites, granulites, gabbros, and peridotites are as a rule weakly magnetic and cannot yield continental lower crust magnetic anomalies
- Only 4 out of 39 sites containing magnetite yield ~0.1 SI *k* values constant until 550°C, compatible with anomalies from continent interiors

Supporting Information:

Supporting Information may be found in the online version of this article.

Correspondence to:

G. Siravo,
gaia.siravo@ingv.it

Citation:

Siravo, G., Speranza, F., Minelli, L., Zucali, M., Fazio, E., Caricchi, C., & Spagnuolo, L. (2025). Magnetic and paleomagnetic characterization of the Ivrea-Verbano lower crust body (NW Italy): Assessing the magnetization of Variscan-age lower crust. *Journal of Geophysical Research: Solid Earth*, *130*, e2024JB031017. https://doi.org/10.1029/2024JB031017

Received 18 DEC 2024
Accepted 20 MAY 2025

Author Contributions:

Conceptualization: Fabio Speranza
Formal analysis: Gaia Siravo, Fabio Speranza, Liliana Minelli, Michele Zucali, Eugenio Fazio, Chiara Caricchi, Lilla Spagnuolo
Investigation: Gaia Siravo, Fabio Speranza
Resources: Fabio Speranza
Writing – original draft: Gaia Siravo, Fabio Speranza, Liliana Minelli, Michele Zucali
Writing – review & editing: Eugenio Fazio

Abstract The source of high-intensity magnetic anomalies from (mostly Precambrian) lower crust of continent interiors has long been debated, as it requires speculative rocks yielding 2–6 A/m magnetization. We report on the magnetic and paleomagnetic investigation of the Ivrea-Verbano Zone (IVZ), Western Alps, where metamorphic and intrusive lower crust rocks of Late Variscan-Permian ages are exposed. We sampled 39 oriented sites along the Cannobina, Ossola, Strona, and Sesia valleys/sections. Low ($0.27–2.1 \cdot 10^{-3}$ SI) magnetic susceptibility (k) values were measured in metapelite-metabasite metamorphic rocks from the Ossola and Strona valleys. There only two metabasite (one amphibolite and one granulite) out of 25 metamorphic sites containing pseudo-single domain (PSD) magnetite yield $0.48–1.1 \cdot 10^{-1}$ SI k values that remain constant until 550°C heating. K of gabbros-granodiorites from Sesia valley mimic low values from metamorphic rocks, whereas at Cannobina valley one gabbro and one mafic granulite display values comparable to the two strongly magnetic sites from Ossola/Strona valleys. Peridotite lenses at Balmuccia and Finero similarly yielded low ($0.24–5.5 \cdot 10^{-3}$ SI) k values, consistently with their low (<20%) serpentinization. Remanence contribution is negligible, as (a) $Q < 1$ values imply remanent magnetization subordinate to induced magnetization, (b) paleomagnetic directions from most magnetic sites are scattered, and (c) remanence is unstable at lower crust temperatures. We conclude that IVZ lower crust rocks could not yield magnetic anomalies generated by Precambrian lower crust from continent interiors, and similar conclusions might stand for other Variscan-age lower crust sections. Scattered high-intensity metabasites could be candidates, if their PSD magnetite-rich mineralogy dominated Precambrian lower crust.

Plain Language Summary The interior of stable and old (>600 Ma) continental areas, hide the source of high-intensity magnetic anomalies. Crustal magnetic anomalies are measured by airborne surveys and indicate that a certain rock is rich in strongly magnetic minerals (mainly magnetite) as to produce a local field that may add or subtract to (depending on magnetization direction of the source rock) to the local Earth's magnetic field. The source of such anomalies is a matter of debate as the potential sources are normally hidden at 20–40 km depths below continents. In the western Alps, one of the most complete lower crust sections has been exhumed due to Alpine orogenesis and is exposed in the Ivrea Verbano Zone. We sampled and measured the magnetic properties of Late Variscan-Permian metamorphic and intrusive lower crust rocks at 39 sites along the Cannobina, Ossola, Strona, and Sesia valleys/sections. Results indicate that the Ivrea Verbano lower crust body definitely could not yield lower crust magnetic anomalies.

1. Introduction

The progressive acquisition of airborne and satellite magnetic data made clear in the 1980s that the strongest magnetic anomalies (intensity > 300 nT) of Earth are found above Precambrian continental interiors (Frost and Shive, 1986; Schlinger, 1985; Shive, 1989; Shive & Fountain, 1988; Shive et al., 1992). Spectral analysis of magnetic residuals and the lack of exposed or shallow highly magnetic rocks pointed to a hidden and speculative magnetic source laying at lower crust (30–40 km) depths. Internal parts of continents are very cold, and in fact a low average geothermal gradient of some 10°–15°C/km is required for rocks at 30–40 km depths for being colder than ~580°C—the Curie temperature of magnetite, the most common magnetic crustal mineral—thus being able to yield significant magnetization (Lanza and Meloni, 2006). The peridotite of anhydrous mantle is virtually non-magnetic, as iron forms paramagnetic olivine and pyroxene, and no magnetite occurs (Belley et al., 2009; Oufi et al., 2002; Wasilewski and Mayhew, 1982, 1992). Thus the missing magnetic source of continent interiors has been mostly located within the lower crust, and associated with (a) mafic magnetite-rich granulites (Brown et al., 2014; Dunlop et al., 2010; Schlinger, 1985), (b) huge gabbro sill-like bodies yielded by basaltic magma underplating at the base of the crust (Mancinelli et al., 2022), (c) magnetite-rich serpentinites derived from peridotite hydration (Rochette, 1994), (d) hematite-ilmenite lamellae (McEnroe et al., 2007; Robinson et al., 2002), and (e) metal alloys (Frost & Shive, 1986; Shive et al., 1992).

The composition, structure, magnetic, minero-petrological and geochemical properties of the continental lower crust are certainly among the most elusive and debated characteristics of the whole external shell of the Earth (Christensen & Mooney, 1995; Gao, Luo, et al., 1998; Gao, Zhang, et al., 1998; Hacker et al., 2015; Holbrook et al., 1992; Rudnick & Fountain, 1995; Rudnick & Gao, 2003, 2014). Most of our knowledge on this topic derives from indirect constraints provided by seismic wave speeds models where velocities are related to different lithologies (e.g., Fountain, 1976). On the other hand, direct information on continental lower crust lithology and magnetic mineralogy is achieved by studying (a) deep-crustal xenoliths lifted at surface by volcanic eruptions (Ferré et al., 2014, 2021; Huang et al., 2013; Rudnick & Fountain, 1995; Rudnick & Gao, 2003, 2014; Wasilewski & Mayhew, 1982, 1992) or, (b) exhumed lower crustal sections (Belluso et al., 1990; Dunlop et al., 2010; Fountain & Salisbury, 1981; Fountain et al., 1990; Percival et al., 1992).

Some lower crust section were exhumed and are exposed, namely the Kohistan sequence of Pakistan (Miller & Christensen, 1994), the Wutai Jining terrain of northern China (Kern et al., 1996; Zhai et al., 2001), the Vredefort dome and Kaapvaal craton of South Africa (Hart et al., 1990; Tredoux et al., 1999), the Musgrave range of central Australia (Fountain & Salisbury, 1981; Percival et al., 1992), the Bamble sector of southern Norway (Pinet & Jaupart, 1987), the southern Alaska (Talkeetna section, Pearcy et al., 1990), and the Archean Canadian shield (Kapuskasing uplift, Fountain et al., 1990; Shaw et al., 1994 and Pikwitonei, Dunlop et al., 2010; Fountain & Salisbury, 1981; Percival & Card, 1983). However, the likely more complete and less tectonically disturbed continental lower crust section exposed on Earth is the Ivrea-Verbano Zone (IVZ), considered as a global petro-geophysical reference due to favorable exposure and little or no metamorphic retrogression (Fountain, 1976; Mehnert, 1975; Pistone et al., 2020 and references therein). The IVZ hosts both a Variscan metamorphic complex and a huge gabbro body (Mafic Complex) that was interpreted as related to basaltic magma batches underplating the crust-mantle interface during the early Permian. Moreover, several peridotitic lenses occur embedded in the metamorphic and gabbro sequence in the IVZ, most notably the Finero and Balmuccia bodies (Figure 1).

Magnetic properties of IVZ rocks have been investigated since long ago but generally considering few sampling points and measuring only magnetic susceptibility (k) values, thus disregarding natural remanent magnetization (NRM) intensity and paleomagnetism (Wagner & Mueller, 1984; Wasilewski & Fountain, 1982; Wasilewski & Warner, 1988). Belluso et al. (1990) provided a rather complete paleomagnetic analysis of 153 samples from IVZ, but individual sample relations between magnetism and metamorphic degree and/or petrography were not addressed in detail. Belluso et al. (1990) concluded that serpentinites and gabbros could yield regional magnetic anomalies above the IVZ, but that their magnetism was too weak to represent the source of long-wavelength magnetic anomalies observed on Precambrian continental crust.

Here we report on a magnetic and paleomagnetic analysis of 312 oriented samples from 39 sites spread along two metamorphic (Val d'Ossola and Val Strona), and two mafic (Val Cannobina and Val Sesia) sections (Figure 1). Magnetic measurements were coupled to petrographic characterization to verify possible correlation between magnetic and mineralogic characteristics. Our work shows that the IVZ rocks are definitely unable to yield magnetic anomalies observed over Precambrian continental interiors, that most gabbros are weakly to moderately magnetic, and serpentinites are virtually lacking as exposed peridotites underwent negligible serpentinization.

2. Characteristics of Cratonic Lower Crust and of the IVZ

Generally, the lower crust is composed of a mixture of igneous and metamorphic rocks, ranging in composition from gabbro to granite (Gao, Zhang, et al., 1998; Hacker et al., 2011; Huang et al., 2013; Rudnick & Gao, 2003, 2014). According to Fountain et al. (1990), typical lower crust features and variations along with increasing depth are (a) an increase of metamorphic grade, from greenschist to granulite facies (Fountain & Salisbury, 1981; Weber et al., 2002); (b) an increase of paleo-pressure, corresponding to a depth range between 15 and 30 km; (c) an increase of mafic lithologies; (d) an increase of magnetization; (e) an increase of density, from 2.6 g/cm^3 of

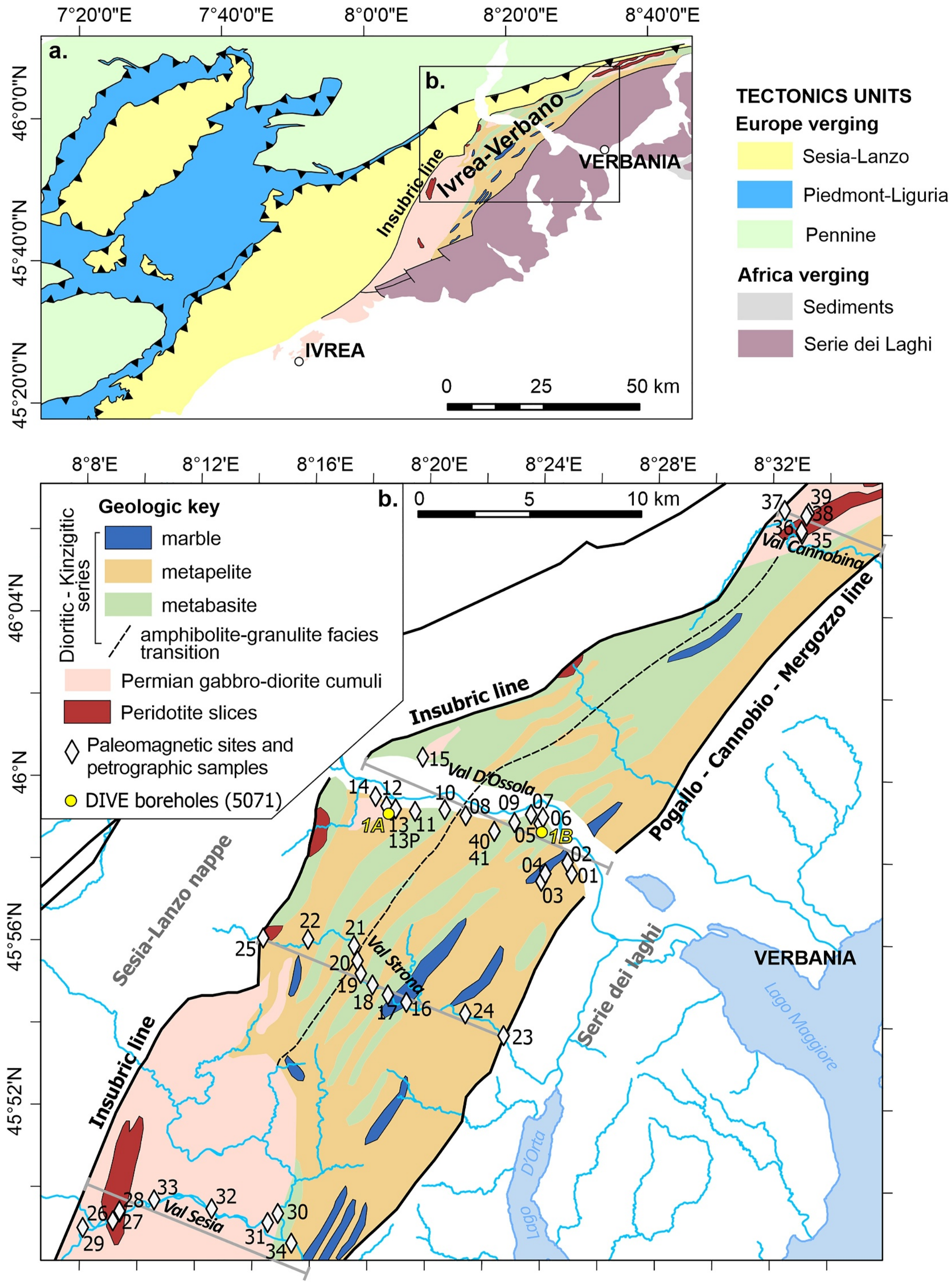

Figure 1. Tectonic units of the Western/Southern Alps (a) and, magnetic, paleomagnetic and petrographic sampling of the Ivrea-Verbano Zone (IVZ) (b). Notice that the metamorphic degree gradually increases form amphibolitic to granulitic moving NW-ward across the IVZ.

felsic granulites to 3.3 g/cm^3 of pyroxenites and peridotites; (f) an increase of P-wave velocity—depending upon rocks composition—from 6.4 to 7.2 km/s; (g) a decrease of content of heat-producing elements (Heier, 1973).

The IVZ stands right at the boundary between Europe- and Africa-verging units of the western Alps (Figure 1), arising from late Cretaceous-Cenozoic collision of Adria—as African promontory—against Europe

(Argand, 1924). The orogen is asymmetric and characterized by a wider and thicker nappe stack verging toward Europe, and a smaller S-SE verging wedge resting above the Adria plate (Bigi et al., 1990; Rosenberg and Kissling, 2013). The so-called Insubric lineament separates Europe- and Adria-verging nappes. In the NW Alps, the IVZ deep crust lens-shaped body (Figure 1) is embedded between the Insubric lineament and the "Serie dei Laghi," formed by upper crust granites, phyllites, Permian volcanics and overlying sediments. The IVZ and the Serie dei Laghi, even though being in tectonic contact, form a rather complete crustal section of the Adria plate margin, completely exposed as regional bedding/foliation is SE-dipping, thus allowing the progressive exposure of originally deeper crust layers moving NW-ward up to the contact with the Insubric lineament (e.g., Brack et al., 2010; Schaltegger & Brack, 2007; Figure 1).

The IVZ comprises two dominant rock units: the Diorite-Kinzigite (or Kinzigite Formation), and the Main Gabbro. Associated with these two units, ultramafic lenticular bodies occur. Diorite-Kinzigites underwent Variscan-age metamorphism (e.g., Handy et al., 1999), as well as a younger Permian high-temperature metamorphic overprint (e.g., Demarchi et al., 1998; Henk et al., 1997).

The Dioritic-Kinzigitic series is made of metapelites and metabasites intercalations with sporadic marbles, best exposed along the Val d'Ossola and Val Strona (Figure 1). From the literature, typical rock types occurring in this area and belonging to metapelite chemical group are kinzigites and stronalites, the first corresponding to sillimanite-garnet bearing gneisses and the second to acid granulites composed mainly by quartz, plagioclase, garnet and pyroxene (e.g., R. Schmid & Wood, 1976). Metabasites are amphibolites composed of plagioclase amphibole, clinopyroxene and garnet or basic granulites composed of plagioclase, ortho- and clino-pyroxene, garnet and minor amphibole. Marbles and silicate rich marbles occur locally as boudins and lenses.

Best exposures of the Main Gabbro are along the Val Sesia and Val Cannobina sections, where granodiorites and gabbros crop out (Figure 1; Quick et al., 1994, 2009; Pressini et al., 2007). Such huge igneous bodies (the Val Sesia body may reach 10 km of thickness for a length exceeding 50 km) belong to the lower Permian (ca. 290 Ma) magmatism, widespread on several Pangea locations, whose geodynamic/tectonic meaning is still debated (e.g., Brack et al., 2010; Doblas et al., 1998; Hoffmann et al., 2013; Lloret et al., 2021; Lützner et al., 2021; Timmerman, 2004; Wilson et al., 2004).

Several ultramafic bodies, occurring as lenses and boudins, are embedded in the IVZ, two of them being at Finero (Val Cannobina) and Balmuccia (Val Sesia, Fountain, 1976; von Raumer et al., 2013; Figure 1). Although Balmuccia lherzolitic peridotites are mostly unaltered, a significant metasomatism has been widely described at the Finero harzburgitic outcrops (Decarlis et al., 2023; Grieco et al., 2001; Zannetti et al., 1999). Multiple metasomatism events have been dated between 290 and 180 Ma, where the younger age should correspond to exhumation as a consequence of Alpine Tethys rifting (De Carlis et al., 2023; Zanetti et al., 1999). Subduction-related metasomatism has been also proposed by several petrological and geochemical investigations (e.g., Cannaò et al., 2022; Hartmann & Wedepohl, 1993; Matsumoto et al., 2005; Morishita et al., 2008; Selverstone & Sharp, 2011; Zanetti et al., 1999).

The IVZ is separated from the Serie dei Laghi unit by the Pogallo and Cannobio-Mergozzo-Brissago faults (Figure 1; Boriani & Giobbi, 2004; S. M. Schmid et al., 1987). The Serie dei Laghi is made of Paleozoic meta-arenites and meta-pelites, intruded by Permian batholiths, mainly of granitic composition, and topped by a thick succession of Permian ignimbrites. The ignimbrites, granites, and the originally underlying Mafic Complex were interpreted to belong to the same early Permian igneous system, sometime also referred to Permian "super-volcano" (Quick et al., 2009).

The exhumation of the IVZ—inferred to originally lie between 15 and 30 km depths—is mainly considered to be the result of Jurassic extension of the Adria margin during Alpine Tethys spreading (e.g., De Carlis et al., 2023; Handy et al., 1999), although later exhumation events also took place (Wolff et al., 2012).

3. Sampling and Methods

We paleomagnetically sampled the IVZ at 39 sites for a total number of 312 oriented samples spread along four sections exposed in the Cannobina, Ossola, Strona, and Sesia valleys (Figure 1; geographic coordinates are reported in Table S1). Each paleomagnetic site has been petrographically characterized by observations at the optical microscope for at least one and up to five thin sections (Table 1 and Figures 2 and 3).

Table 1
Petrographic Characterization of Sampled Paleomagnetic Sites Along the Ivrea-Verbano Zone

	Site	Mineral assemblage	Lithology	Group	Unit	Met.
VAL D'OSSOLA SECTION	IVB01	bt + sil + grt + ms + qz	High-grade gneiss	Metapelite	DK	amp-gran
	IVB02	bt + sil + grt + ms + qz	High-grade gneiss	Metapelite	DK	amp-gran
	IVB03	bt + sil + grt + qz	High-grade gneiss	Metapelite	DK	amp-gran
		bt + sil + grt + qz	High-grade gneiss	Metapelite	DK	amp-gran
	IVB04	amp + cpx + pl + ttn	Amphibolite	Metabasite	DK	amp
		ca + cpx + qz	Marble	Metacarbonates	DK	amp-gran
	IVB05	qz + kfs + grt	High-grade gneiss	Metapelite	DK	gran
		bt + qz + pl + grt	High-grade gneiss	Metapelite	DK	amp-gran
		amp + pl + mag + ilm	Amphibolite	Metabasite	DK	amp
	IVB06	amp + pl + cpx + ttn	Amphibolite	Metabasite	DK	amp
		cpx + pl + amp + ttn	Basic granulite	Metabasite	DK	gran
		amp + pl + cpx + ttn	Amphibolite	Metabasite	DK	amp
	IVB07	amp + pl + cpx + ttn	Amphibolite	Metabasite	DK	amp
	IVB08	cpx + pl + amp + ttn	Basic granulite	Metabasite	DK	gran
	IVB09	amp + pl + cpx + ttn	Amphibolite	Metabasite	DK	amp
		amp + pl + cpx + ttn	Amphibolite	Metabasite	DK	amp
	IVB10	bt + sil + grt + qz	High-grade gneiss	Metapelite	DK	amp-gran
	IVB11	cpx + pl + amp + op	Basic granulite	Metabasite	DK	gran
	IVB12	cpx + opx + pl + amp + op	Basic granulite	Metabasite	DK	gran
		cpx + opx + pl + amp + op	Basic granulite	Metabasite	DK	gran
	IVB13	qz + kfs + grt	High-grade gneiss	Metapelite	DK	amp-gran
		cpx + pl + amp	Basic granulite	Metabasite	DK	gran
	IVB13P	pseudotachylite	High-grade gneiss	–	DK	ukn
	IVB14	cpx + pl + grt + amp + mag + ilm	Basic granulite	Metabasite	DK	gran
		cpx + pl + grt + amp + mag + ilm	Basic granulite	Metabasite	DK	gran
	IVB15	pl + grt + cpx + qtz mylonitic	Basic granulite	Metabasite	DK	gran
		pl + grt + cpx + qtz mylonitic	Basic granulite	Metabasite	DK	gran
VAL STRONA SECTION	IVB16	calc-silicates	Marble	Metacarbonates	DK	amp-gran
	IVB17	amp + pl + cpx + ttn	Amphibolite	Metabasite	DK	amp
		amp + cpx + pl + ttn	Amphibolite	Metabasite	DK	amp
	IVB18	qz + grt + pl + sil + rt	Acid granulite	Metapelite	DK	gran
		sil + grt + qz	High-grade gneiss	Metapelite	DK	gran
		qz + kfs	High-grade gneiss	Metapelite	DK	amp-gran
		amp + cpx + pl + ttn	Amphibolite	Metabasite	DK	amp
	IVB19	bt + sil + grt + qz	High-grade gneiss	Metapelite	DK	amp-gran
		amp + cpx + pl + ttn	Amphibolite	Metabasite	DK	amp
		amp + cpx + pl + ttn	Amphibolite	Metabasite	DK	amp
		amp + pl + cpx + mag + ilm	Amphibolite	Metabasite	DK	amp
	IVB20	amp + pl + cpx + mag + ilm	Amphibolite	Metabasite	DK	amp
	IVB21	bt + qz + pl + grt	High-grade gneiss mylonitic	Metapelite	DK	amp-gran
		bt + qz + pl + grt	High-grade gneiss mylonitic	Metapelite	DK	amp-gran
	IVB22	qz + grt + pl + sil + rt	Acid granulite	Metapelite	DK	gran
		qz + grt + pl + sil + rt	Acid granulite	Metapelite	DK	gran
	IVB23	bt + sil + grt + qz	High-grade gneiss	Metapelite	DK	amp-gran
	IVB24	bt + sil + grt + qz	High-grade gneiss	Metapelite	DK	amp-gran

Table 1
Continued

	Site	Mineral assemblage	Lithology	Group	Unit	Met.
	IVB25	cpx + opx + pl + amp + grt	Basic granulite	Metabasite	DK	gran
VAL SESIA SECTION	IVB26	cpx + ol + sp	Peridotite lherzolites	UM	UM	–
	IVB27	cpx + ol + sp	Peridotite lherzolites	UM	UM	–
	IVB28	ol + cpx + omp + sp	Peridotite lherzolites	UM	UM	–
	IVB29	amp + pl + chl + ep + mag + ilm	Gabbro	Intrusive	MC	–
	IVB30	amp + pl + cpx + op	Gabbro	Intrusive	MC	–
	IVB31	amp + bt + pl	Granodiorite	Intrusive	MC	–
	IVB32	cpx + opx + pl + amp + grt	Basic granulite	Metabasite	DK	gran
	IVB33	cpx + opx + pl + amp + op	Basic granulite	Metabasite	DK	gran
	IVB34	bt + sil + grt + qz	High-grade gneiss	Metapelite	DK	amp-gran
		bt + sil + grt + qz	High-grade gneiss	Metapelite	DK	amp-gran
		amp + cpx + pl + ttn	Amphibolite	Metabasite	DK	amp
		bt + sil + grt + qz	High-grade gneiss	Metapelite	DK	amp-gran
		bt + sil + grt + qz	High-grade gneiss	Metapelite	DK	amp-gran
VAL CANNOBINA SECTION	IVB35	gabbro + mag + ilm	Gabbro foliated	Intrusive	MC	–
		amp + pl + cpx + mag + ilm	Gabbro mylonitic	Intrusive	MC	–
		amp + pl + cpx + mag + ilm + chl + ep	Gabbro	Intrusive	MC	–
	IVB36	amp + pl + cpx + grt + mag + ilm + chl + ep	Gabbro	Intrusive	MC	–
		amp + pl + cpx + grt + mag + ilm + chl + ep	Gabbro mylonitic	Intrusive	MC	–
	IVB37	grt + cpx + amp + mag + ilm	Basic granulite	Metabasite	DK	gran
		grt + cpx + amp + mag + ilm	Basic granulite	Metabasite	DK	gran
	IVB38	cpx + phl	Peridotite harzburgite	UM	UM	–
		ol + phl	Peridotite harzburgite	UM	UM	–
	IVB39	cpx + ol + amp + srp	Peridotite harzburgite	UM	UM	–

Note. Units are DK: Dioritic-Kinzigitic; UM: Ultramafic; MC: Mafic Complex; Met. is the metamorphic grade amp (amphibolite) and gran (granulite). Mineral abbreviations after Whitney and Evans (2010) follows. amp: amphibole; bt: biotite; ca: calcite; chl: chlorite; cpx: clinopyroxene; ep: epidote; grt: garnet; ilm: ilmenite; kfs: k-feldspar; mag: magnetite; ms: muscovite; omp: omphacite; ol: olivine; op: undifferentiated opaque; opx: orthopyroxene; qz: quartz; rt: rutile; sil: silimanite; sp: sphalerite; srp: serpentine; ttn: titanite.

At each site, we collected eight cores using a petrol-powered portable drill cooled by water and oriented them in situ using both a Sun and a magnetic compass, corrected for the local geomagnetic declination in 2020/2023 (∼3°E according to NOAA's National Geophysical Data Center). Foliation attitudes of the Dioritic-Kinzigitic unit —when apparent—were also measured (Table S1).

In the Cannobina valley we sampled two sites in the gabbros, one in mafic granulites and two in the peridotites at Finero (Table 1). In the Sesia valley we sampled one migmatitic metapelite site exposed at the contact between the gabbros and the Dioritic-Kinzigitic complex, two sites in the gabbros, one in the granodiorites, two in mafic granulites and three in the Balmuccia peridotites. In the Dioritic-Kinzigitic rocks from Ossola and Strona valleys we sampled 15 and 10 sites, respectively (Table 1). Along both valleys we sampled five sialic amphibolites (metapelites), six mafic amphibolites (metabasites), one undifferentiated amphibolite, four sialic granulite (metapelites), six mafic granulite (metabasites), one undifferentiated granulite together with two pseudotachylite samples (site 13P), and 2 calc-silicate marble sites.

The drilled cores were cut into standard specimens of 22 mm height, and natural remanent magnetization (NRM) and bulk susceptibility (k) values were measured on each sample. Köenigsberger ratio (Q) diagrams were drawn to estimate relative relevance of remanent versus induced magnetization, considering a local geomagnetic field intensity of 47.7 A/m. Paleomagnetic measurements were done in the shielded room of the "Renato Funiciello paleomagnetic laboratory" at the Istituto Nazionale di Geofisica e Vulcanologia (Rome, Italy), using a 2G Enterprises direct current superconducting quantum interface device cryogenic magnetometer. Alternated-field (AF)

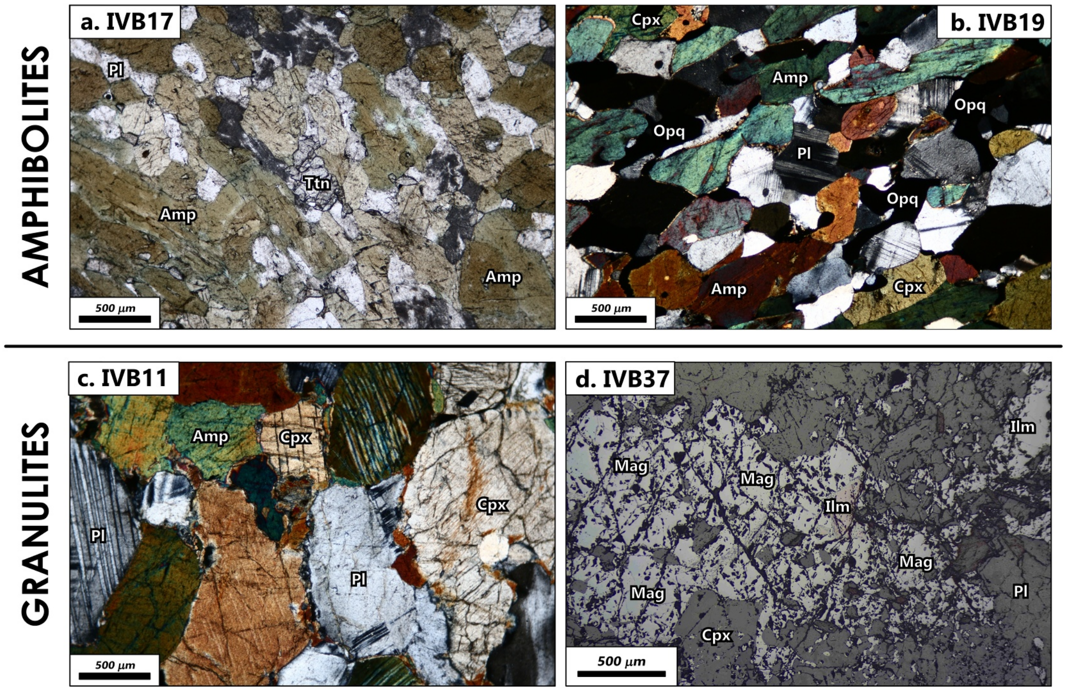

Figure 2. Panoramic microscopic images of collected samples from metabasites (amphibolites and granulites). (a) Titanite-bearing amphibolite from site IVB17 (Val Strona; transmitted light, parallel polarizers); (b) foliated amphibolite from site IVB19 (Val Strona; transmitted light, crossed polarizers); (c) coarse-grained mafic granulite from site IVB11 (Val d'Ossola; transmitted light, crossed polarizers); (d) mafic granulite in reflected light at site IVB37 (Val Cannobina). Reflected light images highlight magnetite (Mag) and ilmenite (Ilm) grains, as both appear opaque in transmitted light. Mineral abbreviations are in Table 1.

demagnetization until 100 mT was performed in 15 steps on every sample from the Val D'Ossola and Val Strona Dioritic-Kinzigitic series. Two representative samples per site, remaining twin specimens from the Dioritic-Kinzigitic series displaying remanence intensity higher than $1.0 \cdot 10^{-1}$ A/m, and all samples from the Mafic and Ultramafic complexes exposed in the Sesia and Cannobina valleys were thermally demagnetized by a Pyrox shielded oven in nine steps up to 600°C.

Demagnetization data were plotted on orthogonal vector diagrams (Zijderveld, 1967), and principal component analysis was used to isolate magnetization components (Kirschvink, 1980). Site-mean paleomagnetic directions were calculated using Fisher's (1953) statistics and plotted on equal-area projections, using the Remasoft software (Chadima & Hrouda, 2006).

Bulk *k* values were measured on all samples using an AGICO Kappabridge KLY-5 bridge. Finally, the magnetic mineralogy was investigated for one representative specimen per sampled lithology by measuring the variation of the low-field magnetic susceptibility during a heating/cooling cycle performed in air, from room temperature up to 700°C using an MFK1-FA Kappabridge coupled with a CS-3 furnace. Empty furnace was measured and corrected for each measured curve. The hysteresis loop parameters that is, the coercive force (Bc, T), the saturation remanent magnetization by mass (Mrs, Am^2/kg) and the saturation magnetization by mass (Ms, Am^2/kg), were determined on small (1 mm^3) rock fragments from the four most magnetic sites and from four sites yielding clustered paleomagnetic directions from both the Mafic Complex and the Dioritic-Kinzigitic series with the vibrating sample magnetometer Lakeshore 8604 up to a field of 1.0 T at steps of 2.5 mT. Ms and Mrs were calculated subtracting the high field linear trend after saturation. The magnetization/coercivity parameters were plotted according to Day et al. (1977).

Volume of all specimens was measured by a hydrostatic balance and used to normalize NRM and *k* values per volume unit, and to calculate density (Table 2). Concerning the 40 peridotite samples from five sites of Finero and Balmuccia, density values were also used to infer the rock serpentinization degree (Table S1), following the linear relation of Miller and Christensen (1997) where serpentinization fraction (S) is inversely related to density (ρ) as:

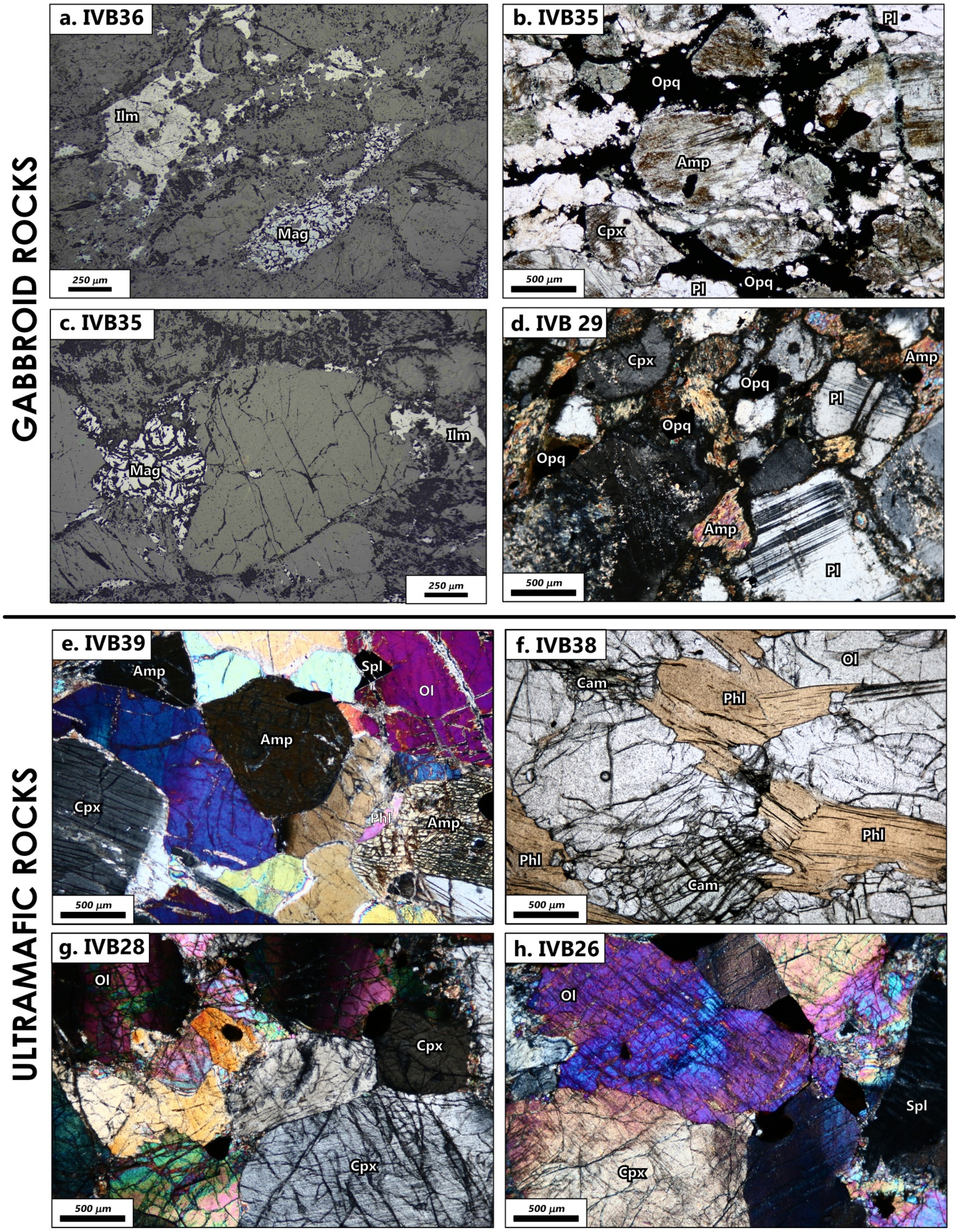

Figure 3. Panoramic microscopic images of gabbros and peridotites in both reflected and transmitted light to identify magnetite (Mag) and ilmenite (Ilm) both appearing as opaque in transmitted light images. (a) Gabbro at site IVB36 (Val Cannobina; reflected light, parallel polarizers); (b) foliated gabbro with high opaque minerals (Opq) content at site IVB35 (Val Cannobina; transmitted light, parallel polarizers); (c) gabbro at site IVB35 (Val Cannobina; reflected light, parallel polarizers); (d) gabbro at site IVB29 (Val Sesia; transmitted light, crossed polarizers); (e) ultramafite consisting of Amp-Cpx-Ol bearing peridotite at site IVB39 (Val Cannobina; transmitted light, crossed polarizers); (f) phlogopite-bearing peridotite at site IVB38 (Val Cannobina; transmitted light, parallel polarizers; Cam: Cromo-amphibole); (g) Ol-Omp-Cpx-Spl-bearing lherzolite at site IVB28 (Val Sesia; transmitted light, parallel polarizers); (h) Cpx-Ol-Spl-bearing lherzolite at site IVB26 (Val Sesia; transmitted light, parallel polarizers). Mineral abbreviations after Whitney and Evans (2010) are listed in Table 1.

Table 2
Paleomagnetic Sites Sampled Along the Ivrea-Verbano Zone and Measured Geophysical Properties

	Site	Lithology syntesis	Density (g/cm^3)	Stand. Dev.	Bulk k (SI)	Stand. Dev.	NRM (A/m)	Stand. Dev.
VAL D'OSSOLA SECTION	IVB01	Sialic amphibolite	2.8656	4.4E − 02	6.0E − 04	1.1E − 04	7.2E − 04	5.7E − 04
	IVB02	Sialic amphibolite	2.6880	2.1E − 02	2.9E − 04	1.9E − 04	9.7E − 02	1.4E − 01
	IVB03	Sialic amphibolite	2.7584	3.2E − 02	3.0E − 04	5.1E − 05	1.9E − 04	1.2E − 04
	IVB04	Marble/Mafic amphibolite	2.7942	3.7E − 02	2.1E − 04	1.5E − 04	2.0E − 02	1.6E − 02
	IVB05	Sialic/Mafic amphibolite	2.7494	1.3E − 01	2.9E − 04	2.0E − 04	5.8E − 03	1.0E − 02
	IVB06	Mafic amphibolite	2.9713	9.8E − 02	7.6E − 04	1.8E − 04	4.8E − 03	3.7E − 03
	IVB07	Mafic amphibolite	3.0073	2.8E − 02	2.1E − 03	1.8E − 03	3.6E − 02	3.3E − 02
	IVB08	Mafic granulite	3.0935	5.9E − 02	1.3E − 03	5.0E − 04	2.7E − 02	2.5E − 02
	IVB09	Mafic amphibolite	3.0086	5.5E − 02	7.4E − 04	1.5E − 04	3.1E − 03	3.8E − 03
	IVB10	Sialic granulite	2.9716	7.2E − 02	5.1E − 04	8.3E − 05	1.9E − 02	4.0E − 02
	IVB11	Mafic granulite	3.0569	1.4E − 01	1.0E − 03	2.3E − 04	1.4E − 02	1.6E − 02
	IVB12	Mafic granulite	3.3138	1.8E − 02	1.0E − 03	2.3E − 04	1.3E − 02	8.0E − 03
	IVB13	Sialic/Mafic granulite	2.8937	8.6E − 02	5.5E − 04	1.4E − 04	5.0E − 03	5.5E − 03
	IVB13P	Pseudotachylite	2.8093	1.4E − 02	4.5E − 04	1.6E − 05	4.7E − 03	1.8E − 03
	IVB14	Mafic granulite	3.1329	6.6E − 02	4.9E − 02	1.3E − 02	3.5E + 00	2.9E + 00
	IVB15	Mafic granulite	3.1272	1.1E − 01	1.1E − 03	5.5E − 04	1.4E − 02	1.2E − 02
VAL STRONA SECTION	IVB16	Marble	2.7066	1.5E − 02	7.1E − 06	1.2E − 05	9.9E − 04	1.6E − 03
	IVB17	Mafic amphibolite	3.0365	2.5E − 02	6.9E − 04	2.7E − 04	1.1E − 02	1.0E − 02
	IVB18	Sialic granulite	2.9099	1.2E − 01	3.2E − 04	1.6E − 04	1.9E − 02	4.5E − 02
	IVB19	Mafic amphibolite	2.9162	8.7E − 02	6.5E − 04	2.2E − 04	3.4E − 03	3.0E − 03
	IVB20	Mafic amphibolite	3.0937	5.1E − 02	1.1E − 01	5.6E − 02	6.1E + 00	5.3E + 00
	IVB21	Sialic granulite	2.9285	7.3E − 02	4.8E − 04	2.4E − 04	1.3E − 01	1.4E − 01
	IVB22	Sialic granulite	2.9261	1.6E − 01	3.8E − 04	2.3E − 04	4.1E − 03	4.5E − 03
	IVB23	Sialic amphibolite	2.7642	3.1E − 02	7.1E − 04	8.6E − 04	2.4E − 02	4.3E − 02
	IVB24	Sialic amphibolite	2.8013	7.4E − 02	5.3E − 04	3.2E − 04	4.1E − 02	6.5E − 02
	IVB25	Mafic granulite	3.0456	4.6E − 02	2.0E − 03	2.0E − 03	3.7E − 02	4.6E − 02
VAL SESIA SECTION	IVB26	Peridotite	3.3923	2.3E − 01	1.1E − 03	5.4E − 04	3.4E − 02	2.6E − 02
	IVB27	Peridotite	3.2197	6.6E − 02	5.5E − 03	4.6E − 03	1.3E − 01	1.4E − 01
	IVB28	Peridotite	3.1937	5.1E − 02	2.7E − 03	1.1E − 03	4.5E − 02	1.2E − 02
	IVB29	Gabbro	2.8395	5.3E − 02	5.9E − 04	2.3E − 04	9.4E − 03	8.2E − 03
	IVB30	Gabbro	2.9571	2.8E − 02	5.7E − 03	7.1E − 03	6.3E − 02	6.7E − 02
	IVB31	Granodiorite	2.9310	4.8E − 02	7.3E − 03	1.1E − 02	6.2E − 02	1.5E − 01
	IVB32	Mafic granulite	2.8128	1.3E − 01	2.0E − 03	1.6E − 03	1.2E − 01	1.4E − 01
	IVB33	Mafic granulite	2.9422	7.0E − 02	6.4E − 04	2.3E − 04	3.7E − 03	3.4E − 03
	IVB34	Metapelite migmatite	2.7803	1.2E − 01	3.2E − 04	2.4E − 04	5.8E − 03	8.8E − 03
VAL CANNOBINA SECTION	IVB35	Gabbro	3.1334	6.3E − 02	1.5E − 01	5.4E − 02	4.2E + 00	2.9E + 00
	IVB36	Gabbro	3.1200	9.3E − 02	2.8E − 02	5.2E − 02	6.7E − 01	1.4E + 00
	IVB37	Mafic granulite	3.1328	3.8E − 02	7.3E − 02	3.4E − 02	5.3E + 00	6.2E + 00
	IVB38	Peridotite	3.2618	1.8E − 02	1.8E − 03	1.1E − 03	1.2E − 02	2.0E − 02
	IVB39	Peridotite	3.2860	2.2E − 02	7.6E − 04	1.2E − 04	8.7E − 03	8.0E − 03

10.1029/2024JB031017

$$S = (3.3 - \rho)/0.785$$

This relation is explained by the hydrothermal (T = 200–400°C) alteration of peridotites, when olivines and pyroxenes are progressively transformed into serpentine family minerals (serpentine and brucite), magnetite, and hydrogen. This process is directly related to density decrease, as olivine and pyroxene have 3.37 and 3.28 g/cm^3 densities, respectively, whereas the reaction product serpentine has a 2.55 g/cm^3 density (O'Hanley, 1996). Bulk densities of unaltered and "fully serpentinized" peridotite fall indeed around 3.3 and 2.6 g/cm^3 values, respectively.

Importantly, serpentinization process yields magnetite, implying simultaneous rise in magnetic susceptibility, and the transformation from non-magnetic (peridotite) to strongly magnetic (serpentinite) rocks (Bonnemains et al., 2016; Cutts et al., 2021; Fichler et al., 2011; Maffione et al., 2014). Rochette (1994) showed that serpentinized peridotite samples from Alpine Tethys oceanic nappes at Lanzo valleys (Piedmont, NW Alps) may exceed 0.1 SI k values, translating to an induced magnetization of ~4 A/m at mid latitudes. He proposed that serpentinites may pretend to the title of "most magnetic rocks existing on Earth." This is probably true only regarding induced magnetization, as remanent magnetization of serpentinites is highly variable in both intensity and directions in the same rock body, and often negligible due to widespread occurrence of multi-domain (MD) magnetite. Conversely, magnetic remanence of basalts is very constant around 5–10 A/m values, and its direction is subparallel to the local geomagnetic field direction occurring during post-eruption lava cooling (Malaguti et al., 2022; Risica et al., 2020, 2022).

4. Results

4.1. Petrology

Five main lithology groups have been recognized by means of optical microscopy (Table 1 and Figures 2 and 3): (a) ultramafic rocks (peridotites); (b) intrusive mafic complex rocks (gabbroids); (c) metapelites (Grt-Bt-Sill gneiss and felsic granulites); (d) metabasites (amphibolites and mafic granulites); (e) meta-carbonates (marbles and calc-silicate rocks). Additionally, brittle Alpine deformation, related to Insubric Line activity, and/or pre-Alpine deformation locally produced mylonites, breccias, and pseudotachylites.

Granulite facies metapelites are essentially felsic granulites with a classic granoblastic texture and gneisses consisting of foliated garnet-, sillimanite-, and biotite-bearing rocks. Metabasites are essentially of two types, amphibolites (Figures 2a and 2b) and granulites (Figures 2c and 2d).

Mafic complex typical rocks are given by gabbros and subordinate granodiorites (Table 1 and Figure 3), predominantly composed of medium-to coarse-grained equigranular amphibole (euhedral), plagioclase (subhedral), ortho- and clino-pyroxene. Interstitial phases are fine-grained plagioclase, amphibole, magnetite, ilmenite, and sulphides, occurring as minor sub-idiomorphic crystals that rim plagioclase and amphibole or constitute a net-textured interconnected phase (e.g., magnetite in Figures 3a–3c).

Usually coarse-grained olivine-pyroxene bearing peridotites display near-120° triple-junctions between grains (Figures 3e and 3f) and show two typical associations in their assemblages: spinel (Figure 3e) or amphibole-phlogopite (Figure 3f). Few olivine grains show serpentinization. Spinel exhibit two distinct forms: the intergranular phase, which occurs between the larger silicates, and the intragranular grain, which typically has a subhedral to euhedral shape and is hosted within the olivines and amphiboles (Figure 3e). Magnetite is most apparent in some gabbros and basic granulites (Figures 2d and 3a–3c), where it occurs as opaque individuals or aggregates between amphibole and pyroxene grains, and subordinately at the edge of amphibole, clinopyroxene or garnet. Reflected light microscopy shows the actual distribution of magnetite with respect to ilmenite (Figures 2d, 3a, and 3c). Magnetite and ilmenite commonly coexist as large aggregates in gabbro samples from Val Cannobina (Figures 3a–3c). They occur as large, elongated aggregates occupying primary igneous features or as thin aggregates marking incipient foliations. Several gabbro samples from Val Cannobina display a predominance of magnetite, which occurs as large aggregates (Figures 3b and 3c) in primary or secondary microdomains (e.g., boudin necks of large hornblende grains). Conversely, gabbro samples from Val Sesia have a very low abundance of magnetite with respect to ilmenite (Figure 3d).

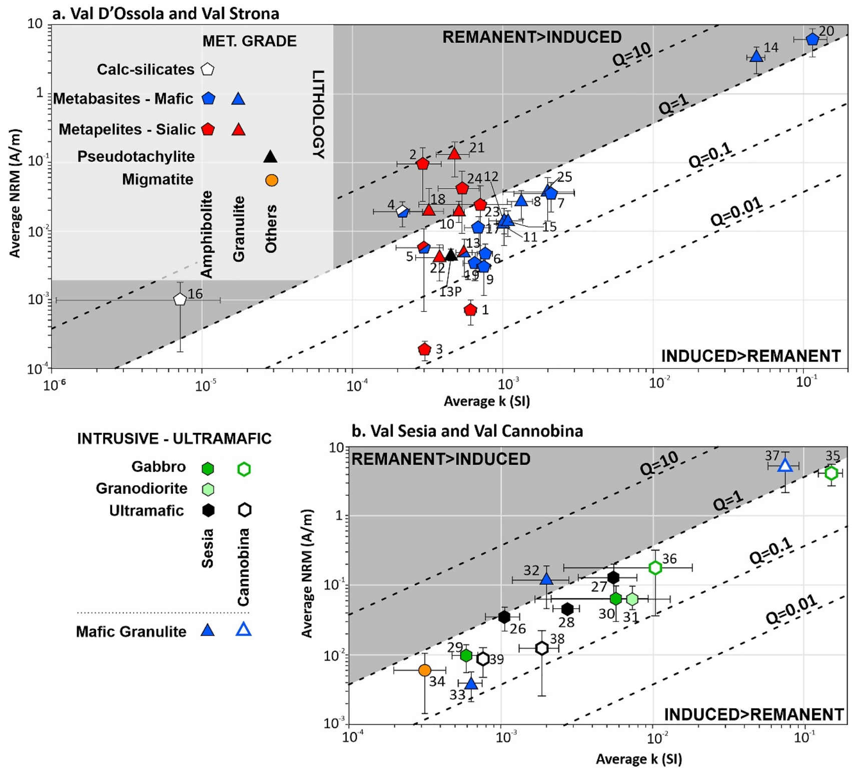

Figure 4. Log-log plot of natural remanent magnetization (NRM) and magnetic susceptibility (*k*) values compared to lines of constant Köenigsberger ratio (Q) calculated for local field of 47.7 A/m from the (a) Val d'Ossola-Val Strona Dioritic-Kinzigitic metamorphic rocks and (b) the Val Sesia-Val Cannobina mostly Mafic and Ultramafic complex.

Magnetite may also occur in basic granulites (Table 1), where it forms aggregates in simplectite microdomains at the boundaries between garnet and clinopyroxene or as large individuals (Figure 2d). In either cases, magnetite coexists with ilmenite or iron sulphides such as pyrite or pyrrhotite.

4.2. Magnetic Properties

The Diorite-Kinzigite metamorphic rocks from the Ossola and Strona valleys yielded as a rule low ($0.29–2.1 \cdot 10^{-3}$ SI) *k* values, invariantly when amphibolitic or granulitic metamorphic grade, and sialic or mafic chemistry are considered (Figure 4a). The pseudotachylite samples (IVB13P) yielded exactly the same (low) *k* values than adjacent parental rocks, and two marble sites yielded very low ($2.1 \cdot 10^{-4}–7.1 \cdot 10^{-6}$ SI) *k* values. Similarly, low ($1.9 \cdot 10^{-4}–1.3 \cdot 10^{-1}$ A/m) NRM values were measured in such rocks. Only exception is observed for one mafic amphibolite and one mafic granulite sites (IVB14 from Ossola and IVB20 from Strona valley), displaying both high *k* ($4.9 \cdot 10^{-2}$ and $1.1 \cdot 10^{-1}$ SI) and NRM (3.5 and 6.1 A/m) values, respectively. Concerning the Köenigsberger ratio Q, most (71%) of the sites yield Q values <1 (Figure 4a), confirming that in high-grade metamorphic rocks induced magnetization prevails over remanent magnetization. It must be noted that the Q values measured on exposed rocks must be considered much greater than those extrapolated on the same rocks located at deeper crustal levels (e.g., Dunlop et al., 2010), as remanence is to be considered highly unstable in geological times at temperature greater than 300–400°C (Pullaiah et al., 1975). Q values slightly >1 were measured in the two strongly magnetic sites IVB14 and IVB20.

Concerning the Sesia Valley, two gabbro and one granodiorite from the Mafic Complex, and two mafic granulites yielded low *k* ($0.59–7.3 \cdot 10^{-3}$ SI) and NRM ($3.7 \cdot 10^{-3}$ to $1.2 \cdot 10^{-1}$ A/m; Figure 4b) values, although higher than those from the Dioritic-Kinzigitic complex exposed in the Ossola and Strona sections. The migmatitic metapelite site (IVB34) sampled at the contact with the Sesia gabbros yielded very low *k* ($3.2 \cdot 10^{-4}$ SI) and NRM ($5.8 \cdot 10^{-3}$ A/m) values. Conversely, higher ($1.5 \cdot 10^{-1}–7.3 \cdot 10^{-2}$ SI) *k* and (4.2–5.3 A/m) NRM values were observed in one gabbro (IVB35) and one mafic granulite (IVB37) sites from the Cannobina valley. Q values from the Sesia and Cannobina rocks are routinely comprised between 0.1 and 1 (Figure 4b).

10.1029/2024JB031017

Peridotite samples yielded low *k* and NRM values that were found to be fully comparable to those of gabbros and diorites from the Sesia valley, with Balmuccia peridotites being about one order of magnitude more magnetic than those from Finero (and all samples showing $Q < 1$ values; Figure 4b). The relation between *k* and density values—hence serpentinization degree of peridotites—will be discussed later.

Susceptibility versus temperature curves of both the Dioritic-Kinzigitic and Mafic complexes showed paramagnetic heating curves and unmatching heating and cooling paths, with *k* values rising significantly during cooling from 600 to 500°C, suggesting magnetite formation during heating (Figure 5a). Although pyrrhotite has been observed in very low concentrations in petrographic and magnetic analyses of samples from both Ossola and Sesia valleys (Belluso et al., 1990; Wasilewski and Warner, 1988), we found no pyrrhotite evidence in the susceptibility versus temperature curves. We infer that little pyrrhotite amount is not enough to be apparent during heating, where *k* is dominated by paramagnetism of amphiboles and pyroxenes. Yet pyrrhotite oxidation is the likely source of magnetite observed in the cooling curves (magnetite has a much greater volume magnetization than pyrrhotite, e.g., Lanza and Meloni, 2006).

A different behavior characterizes the Balmuccia and Finero (Figure 5b) peridotites, the three strongly magnetic metabasites of sites IVB14, IVB20, and IVB37 and the most magnetic gabbro site IVB35 (Figure 5c). The peridotites show clear magnetite occurrence (*k* drop between 500 and 600°C), although the signal is noisy due to the low *k* values. The three strongly magnetic metabasites and the gabbro site IVB35 yield rather reversible curves and a spectacular *k* collapse in only 50°, between 550 and 600°C, suggesting that the magnetic mineralogy is dominated by magnetite. This is in agreement with electronic microscope observations, showing abundant opaque mineral/magnetite occurrence in the four most magnetic sites (Figures 2 and 3).

When plotted in a Day plot (Day et al., 1977; Figure S1 in Supporting Information S1), hysteresis loop parameters from the four most magnetic sites (IVB14, 20, 35 and 37) indicate that pseudo single-domain (PSD) magnetite occurs.

4.3. Paleomagnetism

Most weakly magnetized sites (both the metamorphic and mafic complexes) yielded scattered diagrams (Figures 6a and 6b) and were discarded from further consideration. The most magnetic rocks (sites IVB14, 20, 35, and 37) yielded well-defined characteristic remanent magnetization directions (ChRMs) fully demagnetized at 600°C, thus confirming magnetite occurrence (Figures 6c and 6d). However, individual ChRMs were badly scattered, implying that no mean paleomagnetic directions could be evaluated for such four sites (Figures 6e–6h). Only four sites from various metamorphic rocks and one from the Balmuccia peridotite yielded well-constrained site-mean directions (Figure 6i) defined by ChRMs carried by magnetite (complete demagnetization at 550–600°C) and by hematite at site IVB01 (not fully demagnetized at 680°C; see Figure S2 in Supporting Information S1). Site-mean directions support a negative fold test if the metamorphic foliation is used as tilt proxy. Moreover, the in-situ paleomagnetic directions seem to mirror the post- 200/180 Ma African/Adriatic expected paleomagnetic directions (Torsvik et al., 2012).

Both the four strongly magnetic and paleomagnetically stable sites always show PSD magnetite occurrence (Figure S1 in Supporting Information S1), except for site IVB01 whose magnetic carrier is hematite.

Paleomagnetism of the IVZ thus shows that: (a) the NRM of both amphibolites/granulites and gabbros intruded in the lower crust is routinely weak, and paleomagnetic directions are erratic, thus confirming that remanent magnetization can be disregarded (compared to induced magnetization) when addressing lower crust magnetism; (b) individual paleomagnetic directions of samples from the strongly magnetic sites are well-defined (Figures 6c and 6d), but scattered at the site level (Figures 6e–6h). The reason for such behavior is unclear. As tentative explanation, we may suggest that remanence was acquired during exhumation and cooling at 500–550°C firstly in some magnetite-rich rock volumes (see susceptibility vs. T curves of Figure 5c). Such remanence dipoles distorted the ambient magnetic field in adjacent rock volumes that were magnetized at slightly lower temperatures and/or were less magnetic, yielding paleomagnetic directions deviating significantly from the ambient field direction. In any case, the important implication of these data is that the overall outcrop remanence is minimized by non-parallel remanence vector sums, and this lowers remanence relevance with respect to absolute intensity measured at room temperature. Moreover, at 400–600°C remanence is progressively demagnetized, and Q values extrapolated at lower crust depths are inferred to be significantly lower than those measured at room temperatures

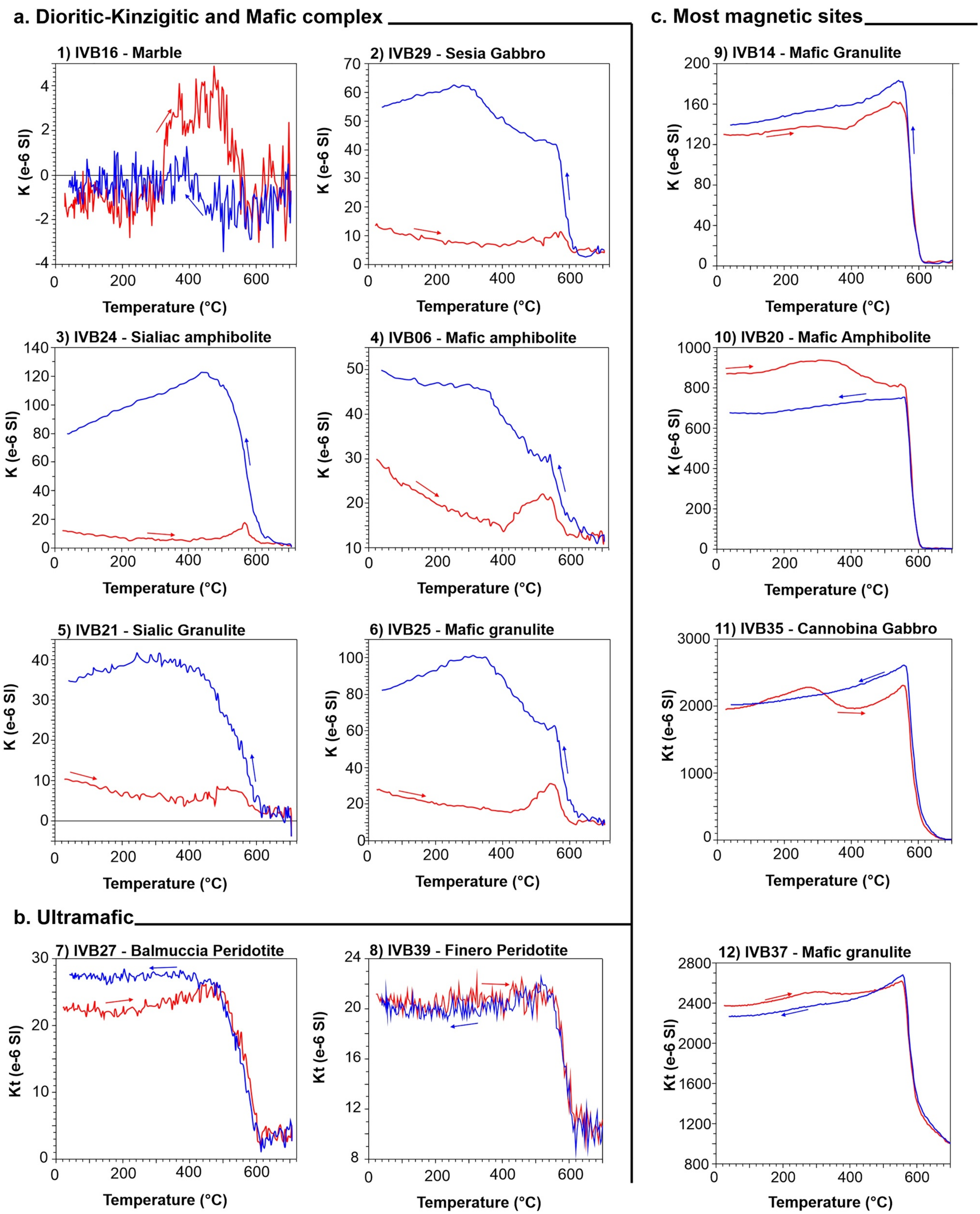

Figure 5. Magnetic susceptibility (*k*) versus increasing/decreasing (red/blue) temperature of one selected specimen per sampled lithology in the Ivrea-Verbano Zone.

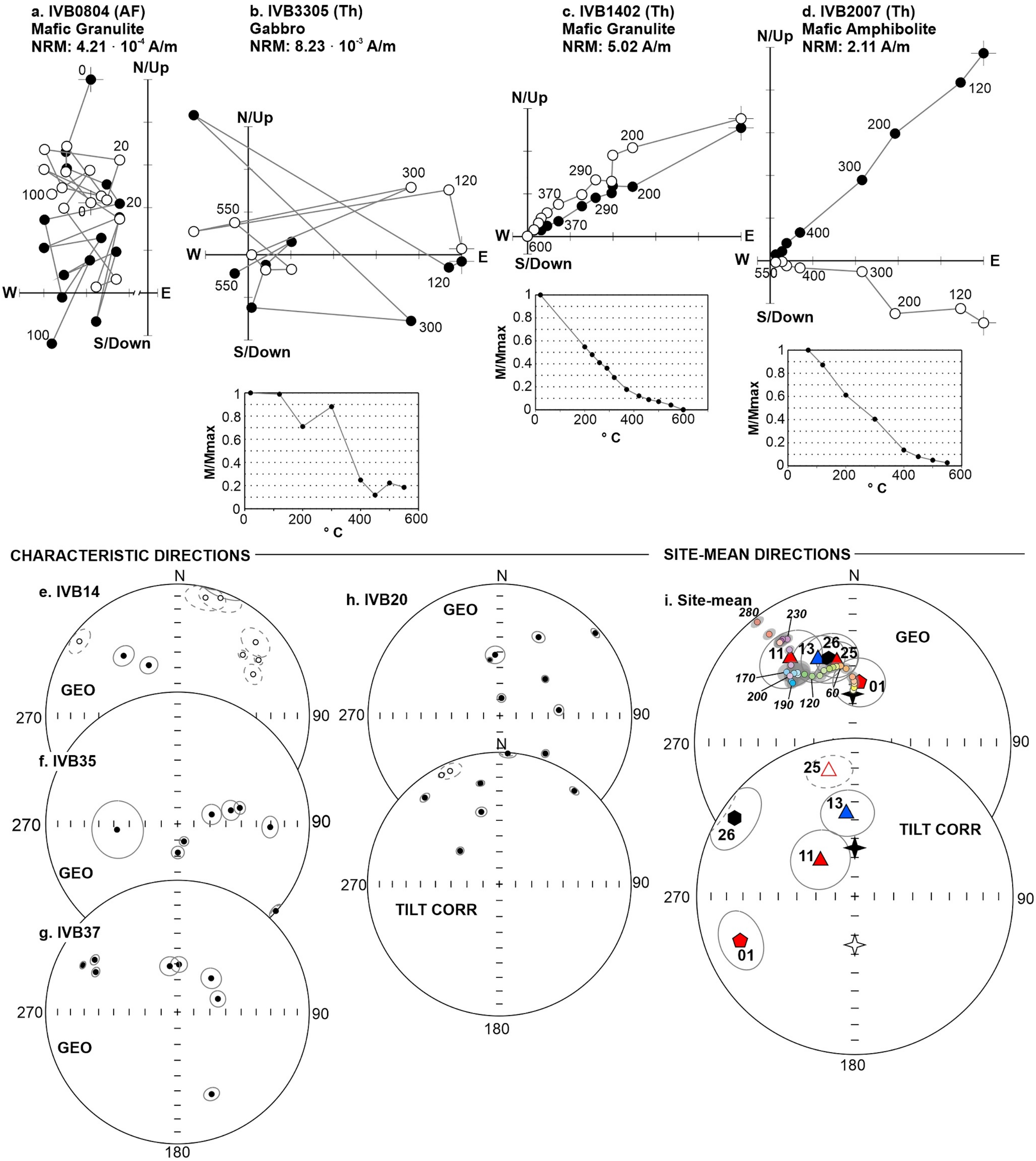

Figure 6. (a–d) Orthogonal vector diagrams of typical demagnetization data, in situ coordinates. Solid and open symbols represent projection on the horizontal and vertical planes, respectively. Demagnetization steps are in mT for alternating field (AF) and in °C for thermal (Th) demagnetization data. Normalized intensity of magnetization versus temperature graphs are reported for thermally treated samples. (e–h) Equal area projection diagrams of characteristic (ChRM) directions from sites IVB14, 35, 37, and 20, respectively. Although these sites have the highest NRM intensity and well defined ChRM directions, site-mean direction is scattered. (i) Site-mean directions from the IVZ together with expected Africa direction at mid Ivrea-Verbano Zone coordinates (lat: 46.0°N; long: 8.3°E) through time. Colors scale is from the geological time scale standard; Ma indicated in italics. Solid and open symbols represent projections on the lower and upper hemisphere, respectively. Stars indicate the expected geocentric axial dipole field direction.

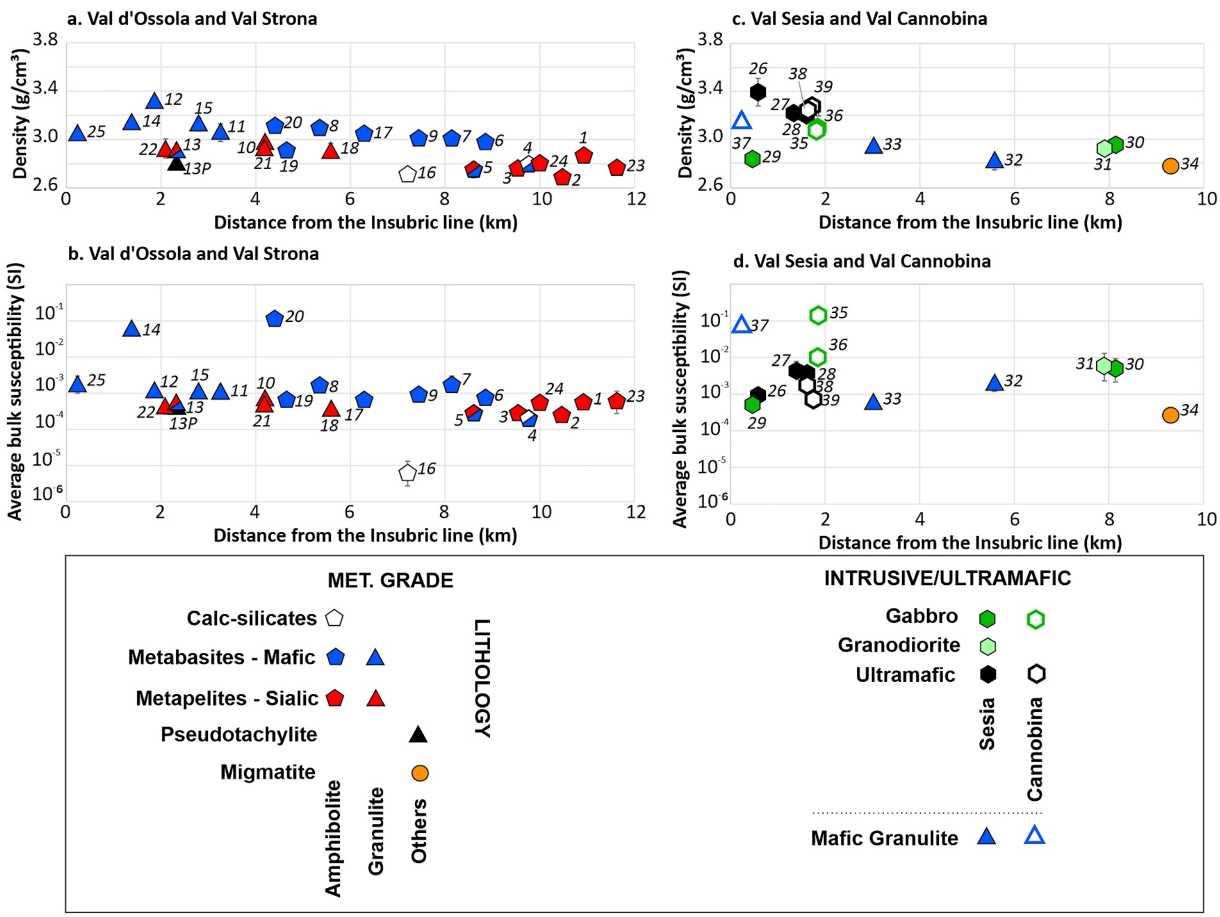

Figure 7. Density and magnetic susceptibility (*k*) values plotted against distance from the Insubric line along sections shown in Figure 1. (a) and (b) Val d'Ossola and Val Strona density and *k*, respectively. (c) and (d) Val Sesia and Val Cannobina density and k, respectively.

(Dunlop et al., 2010). Due to such reasons, remanence is unlikely to play a significant role for lower crust magnetism even when metabasites or gabbros with high (2–5 A/m) NRM values are observed; (c) five sites yielded statistically significant paleomagnetic directions suggesting in situ prolonged remanence acquisition after 200 Ma. This would confirm data by Wolff et al. (2012, and references therein), suggesting that IVZ underwent a first exhumation during Jurassic extensional episodes related to Alpine Tethys spreading.

5. Discussion: Magnetic Trends in the Crust and Serpentinization of the Peridotite Lenses

The relation between metamorphic degree and magnetic properties has been long discussed, being unclear whether there is or not a direct correlation between (both induced and remanent) magnetization intensity and (a) metamorphic grade, (b) density, and (c) mafic/sialic rock chemistry. Here we have the opportunity to evaluate such issues as we collected samples along four valleys/sections roughly orthogonal to IVZ, from the Pogallo lineament, where the IVZ gets in contact with originally shallower crust of Serie dei Laghi, to the Insubric lineament, representing originally deeper crust (Figure 1). In metamorphic Ossola and Strona sections, density rises as expected from ~2.8 g/cm^3 values of sialic amphibolites at SE section margins to 3.0–3.3 g/cm^3 values at 1–2 km from the Insubric lineament, with mafic lithotypes being as a rule denser than sialic samples (Figure 7a). The density and metamorphic degree rise of Ossola and Strona rocks is not however reflected in a similar *k* rise (Figure 7b). Susceptibility stands constant around weak 0.1–2·10^{-3} SI values considering both amphibolites/granulites and mafic/sialic lithotypes, except for the mafic granulite (IVB14; Ossola) and mafic amphibolite (IVB20; Strona) sites where it is higher by about two orders of magnitude from the general trend. The weak susceptibility values are consistent with data from ICDP "Drilling the Ivrea-Verbano zonE" (DIVE) 5071_1_B

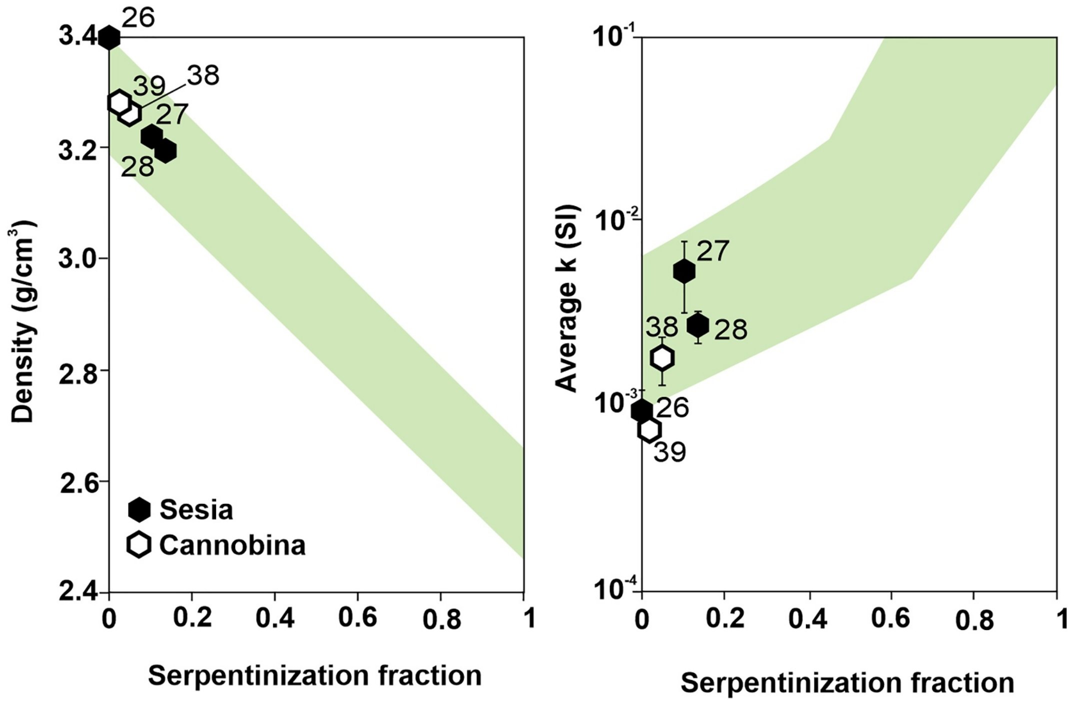

Figure 8. Serpentinization fraction versus average density and magnetic susceptibility (k) values of sampled peridotites. Green areas show the observed serpentinization fraction against density and susceptibility in the data compilation provided by Fichler et al. (2011).

borehole drilled in Val d' Ossola (Figure 1; Li et al., 2024). NRM values are not shown as they are insignificant, being generally weak with erratic demagnetization diagrams, and the two most magnetic sites IVB14 and IVB20 yielded scattered ChRMs (Figures 6e and 6h).

No general rule is apparent to explain the two very magnetic metabasites sites: IVB14 is located in the originally deeper part of the Ossola section, close to the Insubric lineament, whereas IVB20 was sampled in the originally shallower amphibolite-granulite transition horizons of the Strona valley (Figure 1). Such behavior is fully comparable to that documented by Belluso et al. (1990), who showed very weak k values in the metamorphic complex, except two mafic granulite sites from Strona valley yielding the extremely high 0.2 SI k values.

Densities of gabbros/diorites from the Mafic Complex and metabasites in the Sesia Vally section stand rather constantly in the 2.7–3.1 g/cm^3 range, with no trend from the originally shallower to deeper crust sites (Figure 7c). As expected, peridotites are denser and fall in the 3.2–3.4 g/cm^3 density range. In the Sesia valley, k decreases from south-eastern to north-western gabbros-diorites, indicating higher susceptibility in the originally shallower intrusive layers, in turn slightly lower than k value measured on gabbros from Cannobina valley (Figure 7d). This may suggest pristine magnetite differentiation in the original basaltic magma reservoir. K values of the Cannobina gabbro site IVB35 are even greater than typical values of basalts (k = 2–5·10^{-2} SI; Malaguti et al., 2022; Risica et al., 2020, 2022), thus being high enough to provide Precambrian lower crust anomalies (>0.1 k values are needed). Differently than basalts—yielding as a rule very stable and clustered ChRMs—Sesia and Cannobina valley gabbros yielded scattered demagnetization diagrams, likely implying that magma crystallisation at high crustal depths induced changes of the magnetite domain state, from single domain (SD)/PSD to MD.

Susceptibility of peridotites is very low (2.4–3.4·10^{-4} SI) at Finero and low at Balmuccia (1.5–5.5·10^{-3} SI). Peridotite magnetism was compared to serpentinization degree, the latter being evaluated by density values (Figure 8). The serpentinization (Table S1) of samples from both Finero and Balmuccia is low (10%–20%), consistently with low k values.

Our data indicate that the peridotite lenses stacked at the bottom of the IVZ body underwent unsignificant serpentinization, with peridotites from Balmuccia being slightly more serpentinized than those from Finero. Such behavior is unexpectedly opposed to that suggested by petrographic studies, indicating higher metasomatism and alteration at Finero.

Anyway, magnetic properties of IVZ peridotites are greatly different from those of serpentinites from the Lanzo valleys, some 100 km SW of Finero. There, Rochette (1994) studied a mantle slice of the oceanic Liguro-Piedmont nappe, documenting high serpentinization degrees and very high k values, most between 0.4 and $1{\cdot}10^{-1}$ SI. This (rather obviously) shows that oceanic mantle slices embedded in highly deformed far-traveled nappes undergo almost complete serpentinization and become strongly magnetic, whereas virtually in situ continental mantle—or lifted by high-angle faults—escapes hydrothermal alteration and serpentinization.

Thus, it is highly unlikely that serpentinites may exist at the bottom of the continental lower crust and be the source of the intense magnetic anomalies measured there, and this may also have implications for the search of hydrogen reservoirs. Significant hydrogen seepage was recently documented in the Bulqizë chrome mine from the wide Mirdita ophiolite nappe of E Albania (Truche et al., 2024) and inferred to be produced by serpentinization. Such a resource is unlikely to be produced in the lower continental crust of the Adria margin adjacent to the Alps, as peridotite lenses possibly occurring there (as in the IVZ) are not expected to be serpentinized.

The IVZ body, as a part of the Adria margin, overlies an European lithospheric continental slab that has been documented by seismic data until ca. 200 km depths (Lippitsch et al., 2003). In the western US, strong magnetic anomalies were related to the serpentinization of the North America mantle due to fluids released by the underlying subducting Pacific/Juan de Fuca oceanic plates at 50–60 km depths (Blakely et al., 2005). This would imply that fluid release and serpentinization does not occur above subducting continental plates as Europe, and that hydrogen is unlikely to be released in such settings.

Our data and interpretations are mostly consistent with those by Belluso et al. (1990), obtained partly in the same outcrops and based on a 153 oriented samples study compared to the 312 reported by us. They sampled—as we did—the Cannobina, Strona, and Sesia valleys, plus Ivrea and Baldissero (SW part of the Ivrea body), but did not address the Ossola valley. Belluso et al. (1990) did not show k results from individual samples but stated that most susceptive rocks were serpentinized peridotites, gabbros, and two mafic granulite samples from Strona valley. Serpentinized peridotites were sampled at Ivrea and yielded $3{\cdot}10^{-2}$ SI k values, implying a serpentinization degree in the 60% order of magnitude. Only the Ivrea samples among the four peridotite lenses studied by them and us (Finero, Balmuccia, Baldissero, and Ivrea) showed a significant serpentinization degree. Thus, we infer that the Ivrea high serpentinization case is due to local tectonics inducing hydrothermal alteration, and not representative of the IVZ peridotite lenses that are mostly virtually unaltered and yielding very low k values.

6. Conclusions

Magnetic and paleomagnetic analyses carried out at 39 sites (312 oriented samples) spread along the metamorphic (mainly Ossola and Strona valleys) and Mafic—Ultramafic (Cannobina and Sesia valleys) complexes of the Ivrea-Verbano body shed light on the magnetization of Variscan-age continental lower crust, and on the issue of the "missing magnetic source" of Precambrian continent interiors, requiring lower crust magnetizations in the 2–6 A/m range.

Both the metamorphic Dioritic-Kinzigitic complex (invariantly in the amphibolitic/granulitic grades, and sialic/mafic chemistry) and the gabbros/granodiorites yielded as a rule very low ($<2{\cdot}10^{-3}$ SI) to low ($<1{\cdot}10^{-2}$ SI) k values that are totally incompatible with lower crust anomaly sources. In the metamorphic complex, there is definitely no magnetic trend correlated with rise of metamorphic grade (amphibolitic to granulitic) and/or rock chemistry (mafic vs. sialic), although most magnetic sites sampled in the metamorphic complex are metabasites (3 over 10). Magnetic remanence can be definitely neglected as lower crust magnetic source, as even most magnetic sites show scattered directions during thermal demagnetization and/or scattered ChRMs within sites themselves. The reason of ChRM direction scatter within four (tens of m wide) most magnetic sites in unclear, being possibly related with diachronous magnetization acquisition of different rock volumes during rock exhumation and cooling below magnetite Curie temperature (580°C).

Concerning the Mafic complex, only one gabbro site from the Cannobina valley yielded a $1.5{\cdot}10^{-1}$ SI k value that is high enough to account for lower crust magnetism. Our data thus suggest that underplating of huge basaltic bodies at the base of the crust—although certainly a significant lower crust feature, as the 10 km thick Sesia gabbro body testifies—cannot represent the magnetic source of lower crust anomalies of continent interiors.

In the Dioritic-Kinzigitic complex, only the magnetic susceptibility of three metabasites (one in amphibolite and two in the granulite metamorphic grade) is higher and falls in the $0.48–1.1·10^{-1}$ SI range, in agreement with previous results by Belluso et al. (1990). Such values are indeed high enough to translate to an induced magnetization of ~5 A/m that would satisfy the Precambrian lower crust magnetization requirements. The susceptibility versus temperature curves of samples from these sites reveal the occurrence of magnetite yielding remarkably constant (or even increasing) k values until 550°C, and an abrupt k collapse between 550 and 600°C. This implies that such rocks maintain high induced magnetization even at the 400–500°C temperatures required for the lower crust stable continental interiors at 30–40 km depths. The k stability at high temperatures verified by us for few metabasites seems the best evidence explaining a high induced magnetization persisting in hot lower crust needed to explain observed anomalies. Other mechanisms such as Hopkinson peak occurrence (Dunlop, 2014; Hopkinson, 1889) slight rise of magnetite Curie temperature along with hydrostatic pressure (Adams and Green, 1931), and viscous remanent magnetization (Dunlop, 1983; Dunlop & Özdemir, 1990; Shive, 1989) may surely concur with evidence from k/T curves to explain the strong magnetism of lower crust metabasites even at 550°C temperatures.

However, such high magnetization is verified for only three over 10 metabasite sites from the metamorphic IVZ complex, implying that as a whole the Variscan lower crust exposed in the IVZ would be absolutely unable to yield the strong magnetic anomalies measured over Precambrian continental crust. This is consistent with weak and scattered magnetic anomalies observed over Variscan Europe (WDMAM magnetic anomaly map by Choi et al., 2023; Dyment et al., 2015). We conclude that the lithology of Variscan and Precambrian lower crust sections must be strikingly different, the latter being possibly fully composed by the magnetite-rich lithologies observed at the four most magnetic metabasite sites from IVZ. Rock containing high percentage of iron are more abundant in Precambrian than in younger crust (e.g., Simonson et al., 2003; Trendall, 2002), and measurements of Archean iron-rich crust samples yielded extremely high magnetizations, even reaching the astonishing k values of 1 SI (Launay et al., 2018). Widespread iron in Precambrian crust may form ubiquitous PSD magnetite yielding the ~0.1 k values fully stable up to 550°C that we measured in the three more magnetic sites and are needed to generate the magnetic fingerprint of continent interiors.

The magnetization of peridotite lenses embedded in the gabbros both at Balmuccia and Finero is very weak ($k = 0.24–5.5·10^{-3}$ SI), consistently with their low (<20%) serpentinization degrees. This shows that the mantle of continental crust does not undergo serpentinization unless it is detached and far traveled above a nappe pile. Thus, the mantle of continental plates adjacent to paleo-collisional chains—that was only lifted by high-angle faults with negligible tectonic transport—is unlikely to contribute to yield strong magnetic anomalies. Our data also reveal that hydrogen, a byproduct of serpentinization, is unlikely to be produced by peridotite slices embedded in the lower crust of continents, but it requires lifted, deformed, and serpentinized oceanic mantle slices on top of orogenic piles.

Moreover, the subduction of continental mantle/lower crust of the European plate below the Alps and Adria has not released fluids and serpentinized upper plate (Adria) mantle, as it has been inferred to occur in the western US (Blakely et al., 2005). This likely implies that only subducting oceanic crust may release fluids that may hydrothermally serpentinize the overlying upper plate mantle corners. Hydrogen should therefore occur only on orogenic wedges developing above oceanic subduction, whereas continental collision would represent an unfavorable setting.

Acknowledgments
This work was funded by Pianeta Dinamico UNLOCk project (PI Silvia Pondrelli) and INGV. DIVE (Drilling the Ivrea Verbano zonE) project PIs and participants are acknowledged for continuous scientific exchange. Armin Dielforder is acknowledged for providing fruitful information on Val Cannobina outcrops and Domodossola amenities. Marilena Moroni help for thin sections analyses is warmly acknowledged. We feel profoundly honoured that our manuscript was reviewed by so great specialists of rock magnetism and crust magnetization such as David Dunlop, Randy Enkin, Mark Dekkers, and Bjarne Almqvist: to all of them goes our deep gratitude for both reading and commenting our work and publishing along the last decades fundamental works for our formation and scientific growth. Open access publishing facilitated by Istituto Nazionale di Geofisica e Vulcanologia, as part of the Wiley - CRUI-CARE agreement.

Data Availability Statement

Data supporting this work are presented in Tables 1 and 2, Table S1 and reported in Siravo & Speranza, (2024). https://doi.org/10.5281/zenodo.15101810.

References

Adams, L. H., & Green, J. W. (1931). The influence of hydrostatic pressure on the critical temperature of magnetization for iron and other materials. *Terrestrial Magnetism and Atmospheric Electricity*, *36*(3), 161–169. https://doi.org/10.1029/te036i003p00161

Argand, E. (1924). La tectonique de l'Asie. In *Proceedings of the 13th International Geological Congress Brussels* (pp. 171–372).

Belley, F., Ferré, E. C., Martín-Hernández, F., Jackson, M. J., Dyar, M. D., & Catlos, E. J. (2009). The magnetic properties of natural and synthetic $(Fe_x, Mg_{1-x})_2 SiO_4$ olivines. *Earth and Planetary Science Letters*, *284*(3–4), 516–526.

Belluso, E., Biino, G., & Lanza, R. (1990). New data on the rock magnetism in the Ivrea-Verbano zone (Northern Italy) and its relationships to the magnetic anomalies. *Tectonophysics*, *182*(1–2), 79–89. https://doi.org/10.1016/0040-1951(90)90343-7

Bigi, G., Castellarin, A., Coli, M., Dal Piaz, G. V., Sartori, R., Scandone, P., & Vai, G. B., (1990). Structural model of Italy scale 1:500.000, sheet 1. C.N.R., progetto finalizzato geodinamica, SELCA firenze.

Blakely, R. J., Brocher, T. M., & Wells, R. E. (2005). Subduction-zone magnetic anomalies and implications for hydrated forearc mantle. *Geology*, *33*(6), 445–448. https://doi.org/10.1130/g21447.1

Bonnemains, D., Carlut, J., Escartín, J., Mével, C., Andreani, M., & Debret, B. (2016). Magnetic signatures of serpentinization at ophiolite complexes. *Geochemistry, Geophysics, Geosystems*, *17*(8), 2969–2986. https://doi.org/10.1002/2016gc006321

Boriani, A., & Giobbi, E. (2004). Does the basement of Western Southern Alps display a tilted section through the continental crust? A review and discussion. *Periodico di Mineralogia*, *73*(2), 5–22.

Brack, P., Ulmer, P., & Schmid, S. M. (2010). A crustal-scale magmatic system from the Earth's mantle to the Permian surface: Field trip to the area of lower Valsesia and Val d'Ossola (Massiccio dei Laghi, Southern Alps, Northern Italy). *Swiss Bulletin für angewandte Geologie*, *15*(2), 3–21.

Brown, L. L., Webber, J., Williams, M., Regan, S., & Seaman, S. (2014). Magnetism of the lower crust: Observations from the chipman domain, Athabasca granulite terrain, Northern Canada. *Tectonophys*, *624–625*, 66–74. https://doi.org/10.1016/j.tecto.2013.12.004

Cannaò, E., Tiepolo, M., Fumagalli, P., Grieco, G., & Agostini, S. (2022). Metasomatism in the Finero phlogopite peridotite: New insights from C and N concentrations and δ^{13}C-δ^{11}B signatures. *Chemical Geology*, *614*, 121181. https://doi.org/10.1016/j.chemgeo.2022.121181

Chadima, M., & Hrouda, F. (2006). Remasoft 3.0 a user-friendly paleomagnetic data browser and analyzer. *Travaux Géophysiques*, *27*, 20–21.

Choi, Y., Dyment, J., Lesur, V., Garcia, R., Catalan, M., Ishihara, T., et al. (2023). World digital magnetic anomaly map version 2.1. Retrieved from http://www.wdmam.org

Christensen, N. I., & Mooney, W. D. (1995). Seismic velocity structure and composition of the continental crust: A global view. *Journal of Geophysical Research*, *100*(B6), 9761–9788. https://doi.org/10.1029/95jb00259

Cutts, J. A., Steinthorsdottir, K., Turvey, C., Dipple, G. M., Enkin, R. J., & Peacock, S. M. (2021). Deducing mineralogy of serpentinized and carbonated ultramafic rocks using physical properties with implications for carbon sequestration and subduction zone dynamics. *Geochemistry, Geophysics, Geosystems*, *22*(9), e2021GC009989. https://doi.org/10.1029/2021gc009989

Day, R., Fuller, M., & Schmidt, V. A. (1977). Hysteresis properties of titanomagnetites: Grain-size and compositional dependence. *Physics of the Earth and Planetary Interiors*, *13*(4), 260–267. https://doi.org/10.1016/0031-9201(77)90108-x

Decarlis, A., Zanetti, A., Ogunyele, A. C., Ceriani, A., & Tribuzio, R. (2023). The Ivrea-Verbano tectonic evolution: The role of the crust-mantle interactions in rifting localization. *Earth-Science Reviews*, *238*, 104318. https://doi.org/10.1016/j.earscirev.2023.104318

Demarchi, G., Quick, J., Sinigoi, S., & Mayer, A. (1998). Pressure gradient and original orientation of a lower-crustal intrusion in the Ivrea-Verbano zone, Northern Italy. *The Journal of Geology*, *106*(5), 609–621. https://doi.org/10.1086/516045

Doblas, M., Oyarzun, R., Lopez-Ruiz, J., Cebria, J. M., Youbi, N., Mahecha, V., et al. (1998). Permo-carboniferous volcanism in Europe and Northwest Africa: A superplume exhaust valve in the centre of Pangaea? *Journal of African Earth Sciences*, *26*(1), 89–99. https://doi.org/10.1016/s0899-5362(97)00138-3

Dunlop, D. J. (1983). Viscous magnetization of 0.04–100 μm magnetites. *Geophysical Journal International*, *74*(3), 667–687.

Dunlop, D. J. (2014). High-temperature susceptibility of magnetite: A new pseudo-single-domain effect. *Geophysical Journal International*, *199*(2), 707–716. https://doi.org/10.1093/gji/ggu247

Dunlop, D. J., & Özdemir, Ö. (1990). Alternating field stability of high-temperature viscous remanent magnetization. *Physics of the Earth and Planetary Interiors*, *65*(1–2), 188–196.

Dunlop, D. J., Özdemir, Ö., & Costanzo-Alvarez, V. (2010). Magnetic properties of rocks of the Kapuskasing uplift (Ontario, Canada) and origin of long-wavelength magnetic anomalies. *Geophysical Journal International*, *183*(2), 645–658. https://doi.org/10.1111/j.1365-246x.2010.04778.x

Dyment, J., Lesur, V., Hamoudi, M., Choi, Y., Thebault, E., & Catalan, M., & the WDMAM Task Force*, the WDMAM Evaluators**, and the WDMAM Data Providers**. (2015). World digital magnetic anomaly map version 2.0. Retrieved from http://www.wdmam.org

Ferré, E. C., Friedman, S. A., Martín-Hernández, F., Feinberg, J. M., Till, J. L., Ionov, D. A., & Conder, J. A. (2014). Eight good reasons why the uppermost mantle could be magnetic. *Tectonophysics*, *624*(625), 3–14. https://doi.org/10.1016/j.tecto.2014.01.004

Ferré, E. C., Kupenko, I., Martín-Hernández, F., Ravat, D., & Sanchez-Valle, C. (2021). Magnetic sources in the Earth's mantle. *Nature Reviews Earth and Environment*, *2*(1), 59–69.

Fichler, C., Odinsen, T., Rueslåtten, H., Olesen, O., Vindstad, J. E., & Wienecke, S. (2011). Crustal inhomogeneities in the Northern North Sea from potential field modeling: Inherited structure and serpentinites? *Tectonophysics*, *510*(1–2), 172–185. https://doi.org/10.1016/j.tecto.2011.06.026

Fisher, R. A. (1953). Dispersion on a sphere. *Proceedings of the Royal Society of London Series A Mathematical and Physical Sciences*, *217*(1130), 295–305. https://doi.org/10.1098/rspa.1953.0064

Fountain, D. M. (1976). The Ivrea—Verbano and strona-ceneri zones, Northern Italy: A cross-section of the continental crust—New evidence from seismic velocities of rock samples. *Tectonophysics*, *33*(1–2), 145–165. https://doi.org/10.1016/0040-1951(76)90054-8

Fountain, D. M., & Salisbury, M. H. (1981). Exposed cross-sections through the continental crust: Implications for crustal structure, petrology, and evolution. *Earth and Planetary Science Letters*, *56*, 263–277. https://doi.org/10.1016/0012-821x(81)90133-3

Fountain, D. M., Salisbury, M. H., & Percival, J. A. (1990). Seismic structure of the continental crust based on rock velocity measurements from the Kapuskasing uplift. *Journal of Geophysical Research*, *95*(B2), 1167–1186. https://doi.org/10.1029/jb095ib02p01167

Frost, B. R., & Shive, P. N. (1986). Magnetic mineralogy of the lower continental crust. *Journal of Geophysical Research*, *91*(B6), 6513–6521. https://doi.org/10.1029/jb091ib06p06513

Gao, S., Luo, T.-C., Zhang, B.-R., Zhang, H. F., Han, Y. w., Zhao, Z. D., & Hu, Y. K. (1998). Chemical composition of the continental crust as revealed by studies in East China. *Geochimica et Cosmochimica Acta*, *62*(11), 1959–1975. https://doi.org/10.1016/s0016-7037(98)00121-5

Gao, S., Zhang, B.-R., Jin, Z.-M., Kern, H., Luo, T.-C., & Zhao, Z.-D. (1998). How mafic is the lower continental crust? *Earth and Planetary Science Letters*, *106*(1–4), 101–117. https://doi.org/10.1016/s0012-821x(98)00140-x

Grieco, G., Ferrario, A., von Quadt, A., Koeppel, V., & Mathez, E. A. (2001). The zircon-bearing chromitites of the phlogopite peridotite of Finero (Ivrea Zone, Southern Alps): Evidence and geochronology of a metasomatized mantle slab. *Journal of Petrology*, *42*(1), 89–101. https://doi.org/10.1093/petrology/42.1.89

Hacker, B. R., Kelemen, P. B., & Behn, M. D. (2011). Differentiation of the continental crust by relamination. *Earth and Planetary Science Letters*, *307*(3–4), 501–516. https://doi.org/10.1016/j.epsl.2011.05.024

Hacker, B. R., Kelemen, P. B., & Behn, M. D. (2015). Continental lower crust. *Annual Review of Earth and Planetary Sciences*, *43*(1), 167–205. https://doi.org/10.1146/annurev-earth-050212-124117

Handy, M. R., Franz, L., Heller, F., Janott, B., & Zurbriggen, R. (1999). Multistage accretion and exhumation of the continental crust (Ivrea crustal section, Italy and Switzerland). *Tectonics*, *18*(6), 1154–1177. https://doi.org/10.1029/1999tc900034

Hart, R. J., Andreoli, M. A. G., Smith, C. B., Otter, M. L., & Durrheim, R. (1990). Ultramafic rocks in the centre of the Vredefort structure (South Africa): Possible exposure of the upper mantle? *Chemical Geology*, *83*(3–4), 233–248. https://doi.org/10.1016/0009-2541(90)90282-c

Hartmann, G., & Wedepohl, K. H. (1993). The composition of peridotite tectonites from the Ivrea complex, Northern Italy: Residues from melt extraction. *Geochimica et Cosmochimica Acta*, *57*(8), 1761–1782. https://doi.org/10.1016/0016-7037(93)90112-a

Heier, K. S. (1973). A Discussion on the evolution of the Precambrian crust-Geochemistry of granulite facies rocks and problems of their origin. *Philosophical Transactions of the Royal Society of London - Series A: Mathematical and Physical Sciences*, *273*(1235), 429–442.

Henk, A., Franz, L., Teufel, S., & Oncken, O. (1997). Magmatic underplating, extension, and crustal reequilibration: Insights from a cross-section through the Ivrea Zone and strona-ceneri zone, Northern Italy. *The Journal of Geology*, *105*(3), 367–377. https://doi.org/10.1086/515932

Hoffmann, U., Breitkreuz, C., Breiter, K., Sergeev, S., Stanek, K., & Tichomirowa, M. (2013). Carboniferous–Permian volcanic evolution in central Europe—U/Pb ages of volcanic rocks in Saxony (Germany) and Northern Bohemia (Czech Republic). *International Journal of Earth Sciences*, *102*(1), 73–99. https://doi.org/10.1007/s00531-012-0791-2

Holbrook, W. S., Mooney, W. D., & Christensen, N. I. (1992). The seismic velocity structure of the deep continental crust. In D. M. Fountain, R. Arculus, & R. W. Kay (Eds.), *Continental lower crust* (pp. 1–44). Elsevier.

Hopkinson, J. (1889). XIV. Magnetic and other physical properties of iron at a high temperature. *Philosophical Transactions of the Royal Society of London*, *180*, 443–465.

Huang, Y., Chubakov, V., Mantovani, F., Rudkick, R. L., & McDonough, W. F. (2013). A reference Earth model for the heat-producing elements and associated geoneutrino flux. *Geochem. Geophys. Geosyst.*, *14*(6), 2003–2029. https://doi.org/10.1002/ggge.20129

Kern, H., Gao, S., & Liu, Q. S. (1996). Seismic properties and densities of middle and lower crustal rocks exposed along the North China geoscience transect. *Earth and Planetary Science Letters*, *139*(3–4), 439–455. https://doi.org/10.1016/0012-821x(95)00240-d

Kirschvink, J. (1980). The least-squares line and plane and the analysis of palaeomagnetic data. *Geophysical Journal International*, *62*(3), 699–718. https://doi.org/10.1111/j.1365-246x.1980.tb02601.x

Lanza, R., & Meloni, A. (2006). *The Earth's magnetic field* (pp. 1–66). Springer Berlin Heidelberg.

Launay, N., Quesnel, Y., Rochette, P., & Demory, F. (2018). Iron formations as the source of the West African magnetic crustal anomaly. *Frontiers in Earth Science*, *6*, 32. https://doi.org/10.3389/feart.2018.00032

Li, J., Caspari, E., Greenwood, A., Pierdominici, S., Lemke, K., Venier, M., et al. (2024). Integrated rock mass characterization of the lower continental crust along the ICDP-DIVE 5071_1_B borehole in the Ivrea-Verbano Zone. *Geochemistry, Geophysics, Geosystems*, *25*(12), e2024GC011707. https://doi.org/10.1029/2024gc011707

Lippitsch, R., Kissling, E., & Ansorge, J. (2003). Upper mantle structure beneath the Alpine orogen from high-resolution teleseismic tomography. *Journal of Geophysical Research*, *108*(B8). https://doi.org/10.1029/2002jb002016

Lloret, J., López-Gómez, J., Heredia, N., Martín-González, F., de la Horra, R., Borruel-Abadía, V., et al. (2021). Transition between variscan and alpine cycles in the Pyrenean-Cantabrian Mountains (N Spain): Geodynamic evolution of near-equator European Permian Basins. *Global and Planetary Change*, *207*, 103677. https://doi.org/10.1016/j.gloplacha.2021.103677

Lützner, H., Tichomirowa, M., Käßner, A., & Gaupp, R. (2021). Latest carboniferous to early Permian volcano-stratigraphic evolution in central Europe: U–Pb CA–ID–TIMS ages of volcanic rocks in the Thuringian Forest Basin (Germany). *International Journal of Earth Sciences*, *110*(1), 377–398. https://doi.org/10.1007/s00531-020-01957-y

Maffione, M., Morris, A., Plümper, O., & Van Hinsbergen, D. J. (2014). Magnetic properties of variably serpentinized peridotites and their implication for the evolution of oceanic core complexes. *Geochemistry, Geophysics, Geosystems*, *15*(4), 923–944. https://doi.org/10.1002/2013gc004993

Malaguti, A. B., Rosi, M., Pistolesi, M., Speranza, F., & Menzies, M. (2022). The contribution of palaeomagnetism, tephrochronology and radiocarbon dating to refine the last 1100 years of eruptive activity at Vulcano (Italy). *Bulletin of Volcanology*, *84*, 1–19. https://doi.org/10.1007/s00445-021-01515-7

Mancinelli, P., Scisciani, V., Pauselli, C., Stampfli, G. M., Speranza, F., & Vasiljević, I. (2022). Back-arc underplating provided crustal accretion affecting topography and sedimentation in the Adria Microplate. *Marine and Petroleum Geology*, *136*, 105470. https://doi.org/10.1016/j.marpetgeo.2021.105470

Matsumoto, T., Morishita, T., Matsuda, J. I., Fujioka, T., Takebe, M., Yamamoto, K., & Arai, S. (2005). Noble gases in the Finero phlogopite-peridotites, Western Italian Alps. *Earth and Planetary Science Letters*, *238*(1–2), 130–145. https://doi.org/10.1016/j.epsl.2005.07.005

McEnroe, S. A., Robinson, P., Langenhorst, F., Frandsen, C., Terry, M. P., & Boffa Ballaran, T. (2007). Magnetization of exsolution intergrowths of hematite and ilmenite: Mineral chemistry, phase relations, and magnetic properties of hemo-ilmenite ores with micron-to nanometer-scale lamellae from Allard Lake, Quebec. *Journal of Geophysical Research*, *112*(B10). https://doi.org/10.1029/2007jb004973

Mehnert, K. R. (1975). The Ivrea Zone, a model of the deep crust. In *Neues Jahrbuch für Mineralogie, Abhandlungen* (Vol. 125, pp. 156–199).

Miller, D. J., & Christensen, N. I. (1997). Seismic velocities of lower crustal and upper mantle rocks from the slow-spreading Mid-Atlantic Ridge, South of the Kane Transform Zone (MARK). In *Proceedings-Ocean Drilling Program Scientific Results* (pp. 437–456). National Science Foundation.

Miller, D. J., & Christensen, N. L. (1994). Seismic signature and geochemistry of an Island Arc: A multidisciplinary study of the kohistan accreted terrane, Northern Pakistan. *Journal of Geophysical Research*, *99*(B6), 11623–11642. https://doi.org/10.1029/94jb00059

Morishita, T., Hattori, K. H., Terada, K., Matsumoto, T., Yamamoto, K., Takebe, M., et al. (2008). Geochemistry of apatite-rich layers in the Finero phlogopite–peridotite massif (Italian Western Alps) and ion microprobe dating of apatite. *Chemical Geology*, *251*(1–4), 99–111. https://doi.org/10.1016/j.chemgeo.2008.02.018

O'Hanley, D. S. (1996). *Serpentinites: Records of tectonic and petrologic history* (p. 277). Oxford University Press.

Oufi, O., Cannat, M., & Horen, H. (2002). Magnetic properties of variably serpentinized abyssal peridotites. *Journal of Geophysical Research*, *107*(B5), EPM3-1–EPM3-13. https://doi.org/10.1029/2001jb000549

Pearcy, L. G., DeBari, S. M., & Sleep, N. H. (1990). Mass balance calculations for two sections of island arc crust and implications for the formation of continents. *Earth and Planetary Science Letters*, *96*(3–4), 427–442. https://doi.org/10.1016/0012-821x(90)90018-s

Percival, J. A., & Card, K. D. (1983). Archean crust as revealed in the kapuskasing uplift, superior province, Canada. *Geology*, *11*(6), 323–326. https://doi.org/10.1130/0091-7613(1983)11<323:acarit>2.0.co;2

Percival, J. A., Fountain, D. M., & Salisbury, M. H. (1992). Exposed crustal cross sections as windows on the lower crust. In D. M. Fountain, R. Arculus, & R. W. Kay (Eds.), *Continental lower crust: Developments in geotectonics* (pp. 317–362). Elsevier.

Peressini, G., Quick, J. E., Sinigoi, S., Hofmann, A. W., & Fanning, M. (2007). Duration of a large mafic intrusion and heat transfer in the lower crust: A SHRIMP U–Pb zircon study in the ivrea–verbano zone (Western Alps, Italy). *Journal of Petrology*, *48*(6), 1185–1218. https://doi.org/10.1093/petrology/egm014

Pinet, C., & Jaupart, C. (1987). The vertical distribution of radiogenic heat production in the precambrian crust of Norway and Sweden: Geothermal implications. *Geophysical Research Letters*, *14*(3), 260–263. https://doi.org/10.1029/gl014i003p00260

Pistone, M., Ziberna, L., Hetényi, G., Scarponi, M., Zanetti, A., & Müntener, O. (2020). Joint geophysical-petrological modeling on the Ivrea geophysical body beneath Valsesia, Italy: Constraints on the continental lower crust. *Geochemistry, Geophysics, Geosystems*, *21*(12), e2020GC009397. https://doi.org/10.1029/2020GC009397

Pullaiah, G., Irving, E., Buchan, K. L., & Dunlop, D. J. (1975). Magnetization changes caused by burial and uplift. *Earth and Planetary Science Letters*, *28*(2), 133–143. https://doi.org/10.1016/0012-821x(75)90221-6

Quick, J. E., Sinigoi, S., & Mayer, A. (1994). Emplacement dynamics of a large mafic intrusion in the lower crust, Ivrea-Verbano Zone, Northern Italy. *Journal of Geophysical Research*, *99*(B11), 21559–21573. https://doi.org/10.1029/94jb00113

Quick, J. E., Sinigoi, S., Peressini, G., Demarchi, G., Wooden, J. L., & Sbisà, A. (2009). Magmatic plumbing of a large Permian caldera exposed to a depth of 25 km. *Geology*, *37*(7), 603–606. https://doi.org/10.1130/g30003a.1

Risica, G., Di Roberto, A., Speranza, F., Del Carlo, P., Pompilio, M., Meletlidis, S., & Rosi, M. (2020). Refining the holocene eruptive activity at tenerife (Canary islands): The contribution of palaeomagnetism. *Journal of Volcanology and Geothermal Research*, *401*, 106930. https://doi.org/10.1016/j.jvolgeores.2020.106930

Risica, G., Di Roberto, A., Speranza, F., Del Carlo, P., Pompilio, M., Meletlidis, S., & Todrani, A. (2022). Reconstruction of the subaerial Holocene volcanic activity through paleomagnetic and 14C dating methods: El Hierro (Canary Islands). *Journal of Volcanology and Geothermal Research*, *425*, 107526. https://doi.org/10.1016/j.jvolgeores.2022.107526

Robinson, P., Harrison, R. J., McEnroe, S. A., & Hargraves, R. B. (2002). Lamellar magnetism in the haematite–ilmenite series as an explanation for strong remanent magnetization. *Nature*, *418*(6897), 517–520. https://doi.org/10.1038/nature00942

Rochette, P. (1994). Comments on "Anisotropic magnetic susceptibility in the continental lower crust and its implication for the shape of magnetic anomalies" by G. Florio et al. *Geophysical Research Letters*, *21*(24), 2773–2774. https://doi.org/10.1029/94gl02443

Rosenberg, C. L., & Kissling, E. (2013). Three-dimensional insight into Central-Alpine collision: Lower-plate or upper-plate indentation? *Geology*, *41*(12), 1219–1222. https://doi.org/10.1130/g34584.1

Rudnick, R. L., & Fountain, D. M. (1995). Nature and composition of the continental crust: A lower crustal perspective. *Reviews of Geophysics*, *33*(3), 267–309. https://doi.org/10.1029/95rg01302

Rudnick, R. L., & Gao, S. (2003). The composition of the continental crust. In R. L. Rudnick (Ed.), *The crust* (pp. 1–64). Elsevier-Pergamon.

Rudnick, R. L., & Gao, S. (2014). Composition of the continental crust. *Treatise Geochem*, *3*, 1–64. https://doi.org/10.1016/B0-08-043751-6/03016-4

Schaltegger, U., & Brack, P. (2007). Crustal-scale magmatic systems during intracontinental strike-slip tectonics: U, Pb and Hf isotopic constraints from Permian magmatic rocks of the Southern Alps. *International Journal of Earth Sciences*, *96*(6), 1131–1151. https://doi.org/10.1007/s00531-006-0165-8

Schlinger, C. M. (1985). Magnetization of lower crust and interpretation of regional magnetic anomalies: Example from Lofoten and Vesterålen, Norway. *Journal of Geophysical Research*, *90*(B13), 11484–11504. https://doi.org/10.1029/jb090ib13p11484

Schmid, R., & Wood, B. J. (1976). Phase relationships in granulitic metapelites from the Ivrea-Verbano Zone (Northern Italy). *Contributions to Mineralogy and Petrology*, *54*(4), 255–279. https://doi.org/10.1007/bf00389407

Schmid, S. M., Zingg, A., & Handy, M. (1987). The kinematics of movements along the insubric line and the emplacement of the Ivrea zone. *Tectonophysics*, *135*(1–3), 47–66. https://doi.org/10.1016/0040-1951(87)90151-x

Selverstone, J., & Sharp, Z. D. (2011). Chlorine isotope evidence for multicomponent mantle metasomatism in the Ivrea Zone. *Earth and Planetary Science Letters*, *310*(3–4), 429–440. https://doi.org/10.1016/j.epsl.2011.08.034

Shaw, D. M., Dickin, A. P., Li, H., McNutt, R. H., Schwarcz, H. P., & Truscott, M. G. (1994). Crustal geochemistry in the wawa–foleyet region, Ontario. *Canadian Journal of Earth Sciences*, *31*(7), 1104–1121. https://doi.org/10.1139/e94-099

Shive, P. N. (1989). Can remanent magnetization in the deep crust contribute to long wavelength magnetic anomalies? *Geophysical Research Letters*, *16*(1), 89–92. https://doi.org/10.1029/gl016i001p00089

Shive, P. N., Blakeley, R. J., Frost, B. R., & Fountain, D. M. (1992). Magnetic properties of the lower continental crust. In D. M. Fountain, R. Arculus, & R. W. Kay (Eds.), *Continental lower crust* (pp. 145–177). Elsevier.

Shive, P. N., & Fountain, D. M. (1988). Magnetic mineralogy in an Archean crustal cross section: Implications for crustal magnetization. *Journal of Geophysical Research*, *93*(B10), 12177–12186. https://doi.org/10.1029/jb093ib10p12177

Simonson, B. M., Chan, M. A., & Archer, A. W. (2003). *Origin and evolution of large Precambrian iron formations* (pp. 231–244). Special Papers-Geological Society of America.

Siravo, G., & Speranza, F. (2024). Magnetic and paleomagnetic data from the Ivrea-Verbano Zone [Dataset]. *Zenodo*. https://doi.org/10.5281/zenodo.15101810

Timmerman, M. J. (2004). Timing, geodynamic setting and character of Permo-Carboniferous magmatism in the foreland of the Variscan Orogen, NW Europe. *Geological Society, London, Special Publications*, *223*(1), 41–74. https://doi.org/10.1144/gsl.sp.2004.223.01.03

Torsvik, T. H., Van der Voo, R., Preeden, U., Mac Niocaill, C., Steinberger, B., Doubrovine, P. V., et al. (2012). Phanerozoic polar wander, palaeogeography and dynamics. *Earth-Science Reviews*, *114*(3–4), 325–368. https://doi.org/10.1016/j.earscirev.2012.06.007

Tredoux, M., Hart, R. J., Carlson, R. W., & Shirey, S. B. (1999). Ultramafic rocks at the center of the Vredefort structure: Further evidence for the crust on edge model. *Geology*, *27*(10), 923–926. https://doi.org/10.1130/0091-7613(1999)027<0923:uratco>2.3.co;2

Trendall, A. F. (2002). The significance of iron-formation in the Precambrian stratigraphic record. In A. Wladyslaw & L. C. Patricia (Eds.), *Precambrian sedimentary environments: A modern approach to ancient depositional systems* (pp. 33–66).

Truche, L., Donzé, F. V., Goskolli, E., Muceku, B., Loisy, C., Monnin, C., et al. (2024). A deep reservoir for hydrogen drives intense degassing in the Bulqizë ophiolite. *Science*, *383*(6683), 618–621.

Von Raumer, J. F., Bussy, F., Schaltegger, U., Schulz, B., & Stampfli, G. M. (2013). Pre-mesozoic alpine basements—their place in the European paleozoic framework. *Bulletin*, *125*(1–2), 89–108. https://doi.org/10.1130/b30654.1

Wagner, J. J., & Mueller, S. (1984). Geophysical studies of the Ivrea zone—A review. In *Geomagnetic and gravimetric studies of the Ivrea zone* (Vol. 21, pp. 13–20). Geographischer Verlag Berne.

Wasilewski, P., & Fountain, D. M. (1982). The Ivrea Zone as a model for the distribution of magnetization in the continental crust. *Geophysical Research Letters*, *9*(4), 333–336. https://doi.org/10.1029/gl009i004p00333

Wasilewski, P., & Mayhew, M. A. (1982). Crustal xenolith magnetic properties and long wavelength anomaly source requirements. *Geophysical Research Letters*, *9*(4), 329–332. https://doi.org/10.1029/GL009i004p00329

Wasilewski, P., & Mayhew, M. A. (1992). The Moho as a magnetic boundary revisited. *Geophysical Research Letters*, *19*(22), 2259–2262. https://doi.org/10.1029/92GL01997

Wasilewski, P., & Warner, R. D. (1988). Magnetic petrology of deep crustal rocks—Ivrea Zone, Italy. *Earth and Planetary Science Letters*, *87*(3), 347–361. https://doi.org/10.1016/0012-821x(88)90022-2

Weber, M. B., Tarney, J., Kempton, P. D., & Kent, R. W. (2002). Crustal make-up of the Northern Andes: Evidence based on deep crustal xenolith suites, Mercaderes, SW Colombia. *Tectonophysics*, *345*(1–4), 49–82. https://doi.org/10.1016/s0040-1951(01)00206-2

Whitney, D. L., & Evans, B. W. (2010). Abbreviations for names of rock-forming minerals. *American Mineralogist*, *95*(1), 185–187. https://doi.org/10.2138/am.2010.3371

Wilson, M., Neumann, E. R., Davies, G. R., Timmerman, M. J., Heeremans, M., & Larsen, B. T. (2004). Permo-carboniferous magmatism and rifting in Europe: Introduction. *Geological Society*, *223*(1), 1–10. https://doi.org/10.1144/gsl.sp.2004.223.01.01

Wolff, R., Dunkl, I., Kiesselbach, G., Wemmer, K., & Siegesmund, S. (2012). Thermochronological constraints on the multiphase exhumation history of the Ivrea-Verbano Zone of the Southern Alps. *Tectonophysics*, *579*, 104–117. https://doi.org/10.1016/j.tecto.2012.03.019

Zanetti, A., Mazzucchelli, M., Rivalenti, G., & Vannucci, R. (1999). The Finero phlogopite-peridotite massif: An example of subduction-related metasomatism. *Contributions to Mineralogy and Petrology*, *134*(2–3), 107–122. https://doi.org/10.1007/s004100050472

Zhai, M. G., Guo, J. H., & Liu, W. J. (2001). An exposed cross-section of early Precambrian continental lower crust in North China craton. *Physics and Chemistry of the Earth - Part A: Solid Earth and Geodesy*, *26*(9–10), 781–792. https://doi.org/10.1016/s1464-1895(01)00127-2

Zijderveld, J. D. A. (1967). AC demagnetization of rocks: Analysis of results. In *Developments in solid Earth geophysics* (Vol. 3, pp. 254–286). Elsevier. https://doi.org/10.1016/b978-1-4832-2894-5.50049-5